The CIELO Collaboration: Neutron Reactions on ^{1}H, ^{16}O, ^{56}Fe, ^{235,238}U, and ^{239}Pu

M.B. Chadwick,[1,*] E. Dupont,[2] E. Bauge,[3] A. Blokhin,[4] O. Bouland,[5] D.A. Brown,[6] R. Capote,[7] A. Carlson,[8] Y. Danon,[9] C. De Saint Jean,[5] M. Dunn,[10] U. Fischer,[11] R.A. Forrest,[7] S.C. Frankle,[1] T. Fukahori,[12] Z. Ge,[13] S.M. Grimes,[14] G.M. Hale,[1] M. Herman,[6] A. Ignatyuk,[4] M. Ishikawa,[12] N. Iwamoto,[12] O. Iwamoto,[12] M. Jandel,[1] R. Jacqmin,[1] T. Kawano,[1] S. Kunieda,[12] A. Kahler,[1] B. Kiedrowski,[1] I. Kodeli,[15] A.J. Koning,[16] L. Leal,[10] Y.O. Lee,[17] J.P. Lestone,[1] C. Lubitz,[18] M. MacInnes,[1] D. McNabb,[19] R. McKnight,[20] M. Moxon,[21] S. Mughabghab,[6] G. Noguere,[5] G. Palmiotti,[22] A. Plompen,[23] B. Pritychenko,[6] V. Pronyaev,[4] D. Rochman,[16] P. Romain,[3] D. Roubtsov,[24] P. Schillebeeckx,[23] M. Salvatores,[5] S. Simakov,[7] E.Sh. Soukhovitskiĭ,[25] J.C. Sublet,[26] P. Talou,[1] I. Thompson,[19] A. Trkov,[15] R. Vogt,[19] and S. van der Marck[16]

[1] *Los Alamos National Laboratory, Los Alamos, NM 87545, USA*
[2] *Nuclear Energy Agency, OECD, Issy-les-Moulineaux, France*
[3] *CEA, DAM Ile de France, F-91297 Arpajon, France*
[4] *Institute of Physics and Power Engineering, Obninsk, Russia*
[5] *CEA, Nuclear Energy Division, Cadarache, Saint-Paul-lez-Durance, France*
[6] *Brookhaven National Laboratory, Upton, NY 11973-5000, USA*
[7] *International Atomic Energy Agency, Vienna-A-1400, PO Box 100, Austria*
[8] *National Institute of Standards and Technology, Gaithersburg, MD, USA*
[9] *Rensselaer Polytechnic Institute, Troy, NY, USA*
[10] *Oak Ridge National Laboratory, Oak Ridge, TN 37831, USA*
[11] *Karlsruhe Institute of Technology, Karlsruhe, Germany*
[12] *Japan Atomic Energy Agency, Tokai-mura, Japan*
[13] *China Institute of Atomic Energy, Beijing, China*
[14] *Ohio University, Athens, OH 45701, USA*
[15] *Jozef Stefan Institute, Ljubljana, Slovenia*
[16] *Nuclear Research and Consultancy Group, Petten, The Netherlands*
[17] *Korea Atomic Energy Research Institute, Daejeon, South Korea*
[18] *Knolls Atomic Power Laboratory, Schenectady, NY, USA*
[19] *Lawrence Livermore National Laboratory, Livermore, CA, USA*
[20] *Argonne National Laboratory, Argonne, USA*
[21] *Abingdon, Oxfordshire, United Kingdom*
[22] *Idaho National Laboratory, Idaho Falls, ID, USA*
[23] *EC-JRC-IRMM, Geel, Belgium*
[24] *Chalk River Laboratories, AECL, Chalk River, Ontario, Canada*
[25] *Joint Institute for Energy and Nuclear Research, 220109, Minsk-Sosny, Belarus*
[26] *Culham Centre for Fusion Energy, Abingdon, Oxfordshire, United Kingdom*

(Dated: October 4, 2013)

CIELO (Collaborative International Evaluated Library Organization) provides a new working paradigm to facilitate evaluated nuclear reaction data advances. It brings together experts from across the international nuclear reaction data community to identify and document discrepancies among existing evaluated data libraries, measured data, and model calculation interpretations, and aims to make progress in reconciling these discrepancies to create more accurate ENDF-formatted files. The focus will initially be on a small number of the highest-priority isotopes, namely ^{1}H, ^{16}O, ^{56}Fe, ^{235,238}U, and ^{239}Pu. This paper identifies discrepancies between various evaluations of the highest priority isotopes, and was commissioned by the OECD's Nuclear Energy Agency WPEC (Working Party on International Nuclear Data Evaluation Co-operation) during a meeting held in May 2012. The evaluated data for these materials in the existing nuclear data libraries — ENDF/B-VII.1, JEFF-3.1, JENDL-4.0, CENDL-3.1, ROSFOND, IRDFF 1.0 — are reviewed, discrepancies are identified, and some integral properties are given. The paper summarizes a program of nuclear science and computational work needed to create the new CIELO nuclear data evaluations.

* Corresponding author: mbchadwick@lanl.gov

CONTENTS

I. INTRODUCTION

Outstanding progress has been made around the world in nuclear reaction and decay data evaluation. The quality of the main evaluated data libraries, such as ENDF/B-VII.1 [1], JEFF-3.1 [2, 3], JENDL-4.0 [4], BROND/ROSFOND [5], and CENDL-3.1 [6], is high, and for the most part the libraries perform well in neutronics simulations for fission and fusion energy applications (though covariance data that represent uncertainties are less advanced). However, our current understanding is insufficient in many essential areas, some user needs remain inadequately addressed, and a new working paradigm is needed to expedite future evaluated nuclear reaction data advances. We see this as being facilitated by (a) pooling expertise from across the world through creation of collaborative teams, and (b) using new computational techniques for optimization, sensitivity analyses, and uncertainty quantification (UQ). Stronger international collaborations will provide a new framework for nuclear data evaluation, and will help establish the highest fidelity general purpose nuclear database for all nuclear science communities around the world.

It is recognized that for many important applications, for example nuclear criticality calculations, the existing evaluated data perform well in transport simulations owing, in part, to compensating errors in the databases. Different cross section libraries may predict almost the same $k_{\rm eff}$ for benchmark experiments, but for very different reasons at a microscopic level [7, 8]. Such errors must be minimized since simulation predictions away from calibration points (corresponding to the benchmark experiments) can rapidly become erroneous if the underlying physical data used in a simulation are incorrect. Also, cross sections for transmutation reactions, including fission, capture, and $(n, 2n)$, are inadequately known for certain applications. And in many cases scattering cross sections — elastic and inelastic, and secondary neutron energy and angular distributions — are inadequately known for transport calculations.

In this paper we suggest that a new paradigm is needed to more rapidly advance our understanding for the evaluation of nuclear reaction cross sections. Closer international cooperation is needed, where the world's experts for various capabilities are brought together to solve the problems and to provide peer review on proposed solutions. We suggest the name for this collaborative effort, and for the evaluated data libraries that results, be CIELO (Collaborative International Evaluated Library Organization) — the name has the merit of not being closely related to the name of any of the existing evaluation projects, and it emphasizes the centrality of collab-

oration. We anticipate that the OECD's Nuclear Energy Agency and the IAEA's Nuclear Data Section will provide important coordination resources for this project, and the resulting product will be analogous to the "standards cross section files", but for general purpose transport applications (criticality, activation, shielding *etc.*). The principal motivations for CIELO are:

- The product — CIELO — will be higher quality, benefiting from the combined effort of the world's experts in the fields of nuclear data measurement, modeling, evaluation, data processing, and integral validation.
- The scope and complexity of evaluated cross section libraries have become so large that we should consider sharing responsibilities, and resources, for developing the files.
- Such collaborations of experts around the world are less likely to unintentionally omit key measured differential or integral data, or physical insights, in their considerations.
- Errors, and the possibility of poor evaluation decisions, will be minimized through increased peer review. This is particularly important for technical areas where there are few specialists working.
- The diversity of evaluated data libraries has been useful as a tool to communicate open questions regarding our knowledge of cross sections, but new covariances in ENDF, JEFF, JENDL, *etc.* have recently become available, and updated covariances should characterize our uncertainties.
- Pooling our resources to develop high fidelity evaluated data files may help attract new users and key experts who are not typically involved in nuclear data activities.
- The current ENDF, JENDL, JEFF, BROND, and CENDL evaluated data libraries have reached a level of maturity that allows us to prepare the next step that will respond to users' long-term needs of ever more complete and accurate nuclear data for intensive numerical simulations.

Of course, to date cross section evaluation efforts have already benefited in various ways from international collaborations, especially collaborations under the auspices of the IAEA and the WPEC (Working Party on International Nuclear Data Evaluation Co-operation) of the OECD Nuclear Energy Agency. Furthermore, there has been much "borrowing" where one evaluation project has largely, or entirely, adopted an evaluation from another project. So what we are proposing is not new, although it does represent a significant increase in intensity. It is likely that we will need to develop completely new working procedures for effectively and efficiently working together in these international collaborations. This may require establishing a governance model and memoranda of understanding for the participating organizations, though we do not attempt to address such issues here.

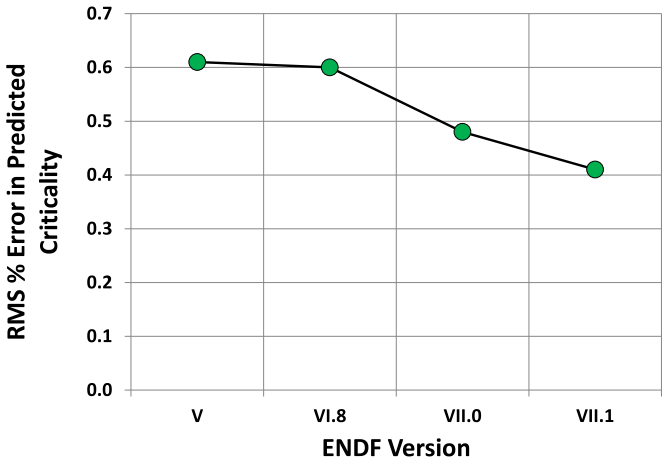

FIG. 1. Calculated/measured root mean square deviation (in %) from unity for nuclear criticality, $k_{\rm eff}$, for a suite of 119 critical assemblies, as a function of ENDF library version number.

One way to measure the overall progress that has been made in advancing the accuracy of evaluated data libraries is to consider comparisons of calculated and measured nuclear criticality ($k_{\rm eff}$). This has been done at Los Alamos for a suite of 119 critical assemblies [9] using the MCNP6 simulation code [10], for various data sets that go back over three decades in time to ENDF/B-V. This suite of critical assemblies includes a selection of all the different neutron spectrum types (fast, intermediate, thermal), actinide materials (HEU, DU, Pu, ...), reflector materials, and so on. The root-mean-square (rms) deviation in C/E from unity is shown as a function of the library version, see Fig. 1. Whilst the error is seen to get smaller with each release of ENDF, it is evident that it is difficult to make substantial improvements with the methods we are presently using – we are facing diminishing returns. CIELO, using new evaluation and optimization methods may enable more significant future improvements. Of course we recognize that considerations of $k_{\rm eff}$ are inadequate to fully quantify the quality of evaluated cross section sets, and one should also look at the evaluated cross sections compared to differential laboratory measurements, where substantial advances have been made over the last decades.

It is useful to list just a few of the successful international collaborative projects that demonstrate the feasibility, and the value, of such efforts.

- The IAEA/WPEC/CSEWG standard effort was comprised of leading researchers from around the world [11]. Some of the resulting standards have been adopted by many projects (e.g. ENDF/B-VII.1, JENDL-4.0, JEFF-3.1), and the IAEA has established a long-term commitment to supporting this effort.

- Several special-purpose nuclear data files have been produced under IAEA coordination, such as the International Reactor Dosimetry and Fusion File (IRDFF) [12], the photonuclear data library, and the Fusion Evaluated Nuclear Data Library (FENDL) [13].

- A new ^{232}Th evaluation was undertaken by an IAEA Coordinated Research Project (CRP) and subsequently adopted by ENDF.

- Evaluations recommended by WPEC's Subgroup 23 (Evaluated Data Library for the Bulk of Fission Products) [14] have been adopted by ENDF, and provide guidance for future evaluations in other projects.

- WPEC Subgroup 4 (^{238}U Capture and Inelastic Cross-sections) [15] helped solve a long-standing problem on the capture cross section in the fast energy range.

- LANL, LLNL, and the CEA have had long-standing collaborations on nuclear reactions in the fast range. Collaborations between ORNL and CEA/Cadarache have also led to jointly developed resonance analyses for many actinides. Two of these, ^{235,238}U, were done under the auspices of WPEC subgroups 18 and 22 in collaboration with Harwell, KAPL, LANL, and other laboratories. ENDF/B-VI Release 5 of ^{235}U was adjusted to calculate HEU thermal solution benchmark eigenvalues correctly, and ^{238}U extended those "targeted" methods to LEU systems. These have been adopted by many other projects. Because the average eigenvalue of uranium-fueled assemblies is now so close to unity, CIELO will have the additional constraint of maintaining that desirable condition.

- The Reference Input Parameter Library (RIPL) [16] illustrates how teams of scientists across the world can come together (under the auspice of the IAEA in this case) to create a valuable reference work summarizing our understanding of nuclear reaction physics.

The first goal of CIELO is shorter term: bringing together experts from across the international nuclear reaction data community to identify discrepancies (and document reasons for the discrepancies) among existing evaluated data libraries, measured data, and model calculation interpretations (described herein), and to make progress in reconciling these discrepancies to create more accurate ENDF-formatted files. The focus will initially be on a small number of the highest-priority isotopes (^{1}H, ^{16}O, ^{56}Fe, ^{235,238}U, ^{239}Pu). If successful, this will subsequently be expanded to include an ever-broadening suite of nuclei. We plan to place the second priority on nuclei such as ^{2}H, ^{6,7}Li, ^{9}Be, ^{10,11}B, ^{12}C, ^{23}Na, ^{52}Cr, ^{58,60}Ni, Mo isotopes, ^{240,241}Pu, and ^{241}Am, but the specifics will be determined later from user community input, from the WPEC High Priority Request List (HPRL), and from priorities identified by WPEC Subgroup 26, 33 and follow-on efforts.

The second goal is for this international collaboration to create demonstrably more accurate evaluations such that the regional efforts (ENDF, JEFF, JENDL, BROND/ROSFOND, CENDL, TENDL *etc.*) will naturally want to adopt CIELO evaluations (or partial evaluations). Over time this may lead to internationally consistent, and internationally maintained, evaluated databases that best represent these constants of nature. But before such a scenario can be planned , we — as an international community — first need to demonstrate that the CIELO concept is indeed feasible.

In this paper we describe the status of existing files in each evaluation project nucleus by nucleus, together with a summary of some outstanding issues that need to be solved. The issues we intend to summarize are: (a) discrepancies amongst the evaluated nuclear data libraries (ENDF, JENDL, JEFF, *etc.*); (b) notable experimental data gaps/discrepancies limiting our understanding; and (c) notable differences in theory and interpretation. In these descriptions, the extent to which the current evaluations already involve much collaboration and borrowing from other evaluations is evident. The thermal cross sections, Westcott factors, resonance integrals, Maxwellian-averaged cross sections (MACS) at 30 keV, and ^{252}Cf(sf) neutron spectrum averaged cross sections, are given in this paper to help identify and illustrate differences and discrepancies.

In addition to this document, we provide a compilation of figures created by the National Nuclear Data Center (NNDC) of BNL in an automated way from the various evaluated databases. As this project evolves, additional figures will be created to help identify and illustrate discrepancies that need to be resolved. This supplement is available to collaborators on the NEA website [17].

Evaluations of cross section uncertainties and correlations (covariances) have become an increasingly important component of nuclear data evaluation work. Such covariance data are important in subsequent studies of the overall uncertainty budget of a neutron transport integrated simulation, for example for criticality or for transmutation rate predictions. There has been much recent work in the nuclear data and transport community on covariances, and the recent releases of evaluated databases include fairly comprehensive covariance data. However, such capabilities are in their early stages and significant improvements are needed to ensure the uncertainties are credible, and complete. CIELO collaborations will include this important topic, although because of limited space we do not address covariances in any detail in this paper.

II. LIGHT ELEMENTS

A. ^{1}H

1. Summary of the evaluations

The n-p cross section is a primary standard in nuclear physics, and the cross section represents a basic tool for studying the nuclear force [11, 18]. The n-p cross section plays an essential role in many neutronics simulations of transport and criticality, as well as absolute measurements of neutron-induced reactions.

The R-matrix analysis for the n-p cross section was performed by G. Hale of LANL as part of the IAEA-WPEC-CSEWG standards effort [11], and it was compiled into the most recent ENDF/B-VII.0 evaluation, which is identical to ENDF/B-VII.1. This was adopted by JENDL-4.0 and ROSFOND. JEFF-3.1 still uses an earlier version of this work from ENDF/B-VI.8. The most recent ENDF/B-VII.0 work by Hale benefits from inclusion of more data (in addition to n-p and p-p data) which includes n-p capture and phototisintegration channels, and Ohio University n-p elastic scattering angular distribution data at 10 MeV [19]. The latter measurement led to ENDF/B-VII.0 upgrades which correct the angular distribution in ENDF/B-VI.8 that had too large a backward-forward center-of-mass (cm) ratio in the angular distribution at 10 MeV.

2. Elastic scattering

As noted above, the existing evaluations have largely converged. Future work will most usefully include further refinements to the R-matrix analysis through the IAEA-WPEC-CSEWG collaboration. Some possibilities are described below.

Some recent high-accuracy angular distribution measurements have been made by Boukharouba *et al.* [19] at Ohio University at 14.9 MeV. The motivation was to better understand this important cross section, and to assess the accuracy of the ENDF/B-VII and phase-shift analysis cross sections. The authors concluded that ENDF/B-VII agrees well with their data, but open questions have hindered a more rigorous test. In particular, very few data have been measured at small cm angles — the lowest-angle data dates from 1967 — and this leads to ambiguities as to whether the shape of the angular distribution monotonically decreases with decreasing angle (P_1 component in the Legendre expanded angular distribution) or whether there is a backward- and forward-angle increase (P_2). Future small-angle precision data are required to help determine this angular distribution cross section to discriminate between the ENDF/B-VII and the Arndt *et al.* and the Nijmegen group predictions [20, 21], and to advance future evaluations. Furthermore, at 14.9 MeV the total elastic scattering cross section in ENDF/B-VII is 1% lower than those of Arndt *et al.* and the Nijmegen group. A more precise determination (1-2%) of both the total and double-differential elastic scattering cross-sections is requested at high incident energy (10-20 MeV) with emphasis on the data at small cm angles (see High Priority Request List at http://www.oecd-nea.org/dbdata/hprl/hprlview.pl?ID=463).

B. ^{16}O

1. Summary of the evaluations

The following description of the oxygen evaluations in use around the world illustrates the interconnected nature of such efforts. The ENDF/B-VII.0 oxygen evaluation, developed by Hale *et al.* at Los Alamos and by Lubitz and Caro (KAPL), has been adopted by many projects. In particular, JEFF-3.1 has adopted this work, which included an upgrade to the (n,α) reaction compared with the earlier ENDF/B-VI.8 file, as has the CENDL-3.1 library. Also, the ROSFOND evaluation adopts ENDF/B-VII.0, though an improvement to radiative capture was made by use of the JENDL-3.3 cross section for capture. And indeed, the new ENDF/B-VII.1 file, although identical to VII.0 in other respects, adopts the JENDL-4.0 capture cross section since ENDF/B-VII.0 needed to be modified to account for deviations away from $1/v$ at higher energies important in nucleosynthesis applications. Although the JENDL-4.0 evaluation is largely independent of the US ENDF work, it did adopt the ENDF/B-VII.0 (n,α) cross section below 6.5 MeV.

2. (n,α) reaction

Discrepancies of up to 30% in both measured and evaluated ^{16}O(n,α) data have been a long-standing issue in the field of fission applications. These discrepancies affect the prediction of $k_{\rm eff}$ for current and innovative reactors, the prediction of helium production in reactors, and the calibration of reference neutron-source strength in metrology measurements. New measurements and evaluations have been requested in the range 2.5-20 MeV to reduce the uncertainty down to 5-10% (see the High Priority Request List and documents therein at http://www.oecd-nea.org/dbdata/hprl/hprlview.pl?ID=417).

The existing ^{16}O(n,α) cross section in ENDF/B-VII.0 and VII.1 is consistent with some data below 6 MeV (the new IRMM and IPPE measurements by Giorginis [22] and the Bair and Haas ORNL data [23] with their recommended 20% decrease) but is discrepant with these new data above 6 MeV. A developmental/test set of multi-channel R-matrix calculations by Hale suggested a fit to data that was about 30% higher for (n,α) in the 3–6 MeV range (in contradiction to the new IRMM/IPPE data) — this was not adopted for VII.1, as it was decided more work is needed to understand this channel.

The (n,α) channel does affect criticality — for example, the lower (n,α) cross section adopted for ENDF/B-VII.0 impacted LCT (Low-enriched-uranium, Compound, Thermal spectrum) benchmarks by increasing $k_{\rm eff}$ slightly [24]. An earlier version of ENDF/B-VI had a higher (n,α) cross section (that is, it better matched the original Bair and Haas data without following their guidance to lower the cross section), and this resulted in H. Huria of Westinghouse finding a lowering of his calculated criticality by 100 – 200 pcm for a commercial reactor design. This led J. Weinman of KAPL to calculate criticality for various homogeneous spheres (in the HST series 1, 9-13, 32, 42, 43) with the result that a decreasing trend as a function of oxygen absorption was observed for ENDF/B-VI.8, but less of a trend was observed for ENDF/B-V. This was part of the reason for Page *et al.* decreasing the (n,α) cross section for ENDF/B-VII.0 (and VII.1). These integral calculations need to be redone, and an assessment made as to whether they can be used to guide evaluation decisions on the (n,α) cross section.

Recently finalized IRMM measured data have been released by Giorginis. The author concludes that ENDF/B-VII.1=VII.0 is accurate below 6 MeV but most likely needs to be modified above 6 MeV (higher from 6.0 to 8.8 MeV; lower above 8.8 MeV, see Fig. 2); the author even provides a scaling factor to apply to ENDF/B-VII.0 above 6 MeV (above 6 MeV the existing ENDF/B-VII.0 evaluation follows earlier ENDF analyses in matching the older US data by Davis *et al.*, but these data are discrepant with the newer Geel-IRMM and IPPE data). The IRMM data are in good agreement with the Harissopulos *et al.* [25] data below 5.2 MeV, but at 6.4 MeV the IRMM data are larger and agree with the corrected Bair and Haas 1973 Oak Ridge data (Bair and Haas recommended a 15–20% reduction to their original data). At 5.4 MeV the IRMM data agree with the IPPE data, but at 6.4 MeV the IPPE data are significantly higher; Giorginis *et al.* suggest that a problem exists with the IPPE data.

Future (n,α) evaluation work on oxygen is needed to address at least two issues. Firstly, as described above there are some discrepancies in the measurements for (n,α) direct and inverse channels. If the recent IRMM data are correct, ENDF needs to be modified above 6 MeV. Secondly, there are R-matrix theory insights that could be in conflict with these IRMM data. The R-matrix analysis by Hale, which is also informed by the total cross section data, presently predicts a higher (n,α) cross section than ENDF for the few MeVs above threshold, as does preliminary R-matrix work by Kunieda and by Leal.

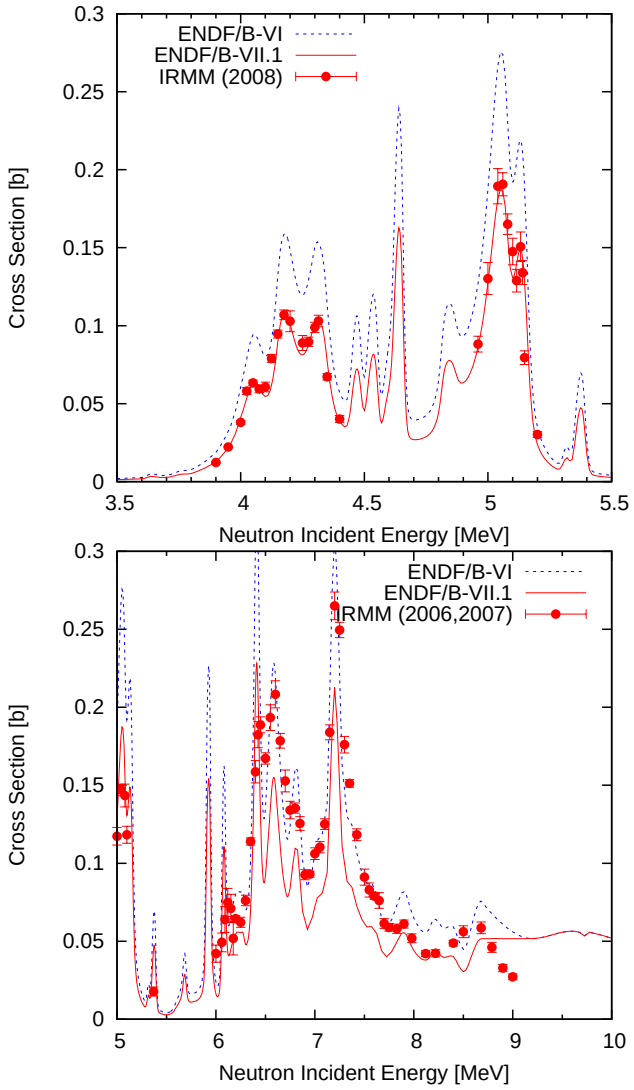

FIG. 2. ^{16}O(n,α) showing recent IRMM measurements by Giorginis *et al.* They suggest that the ENDF/B-VII.1 needs to be increased above 6 MeV. The (n,α_0) cross sections in ENDF/B-VI and ENDF/B-VII.1 are broadened by a Gaussian to reflect the detector response.

3. *Radiative capture*

ENDF/B-VII.1 adopted JENDL-4.0 data from below thermal to higher energies. This was motivated by a desire to have more accurate values above 0.1 keV, especially at 30 keV for nuclear astrophysics applications. The capture data in JENDL include the direct capture and a description of the resonance process performed by Mengoni making use of the Igashira [26] data. JEFF-3.1 and CENDL have not yet adopted this upgrade. As the radiative capture cross section is expected to have a resonance structure for energies above 0.1 MeV, a future upgrade above this energy would be beneficial.

4. *Elastic scattering*

The thermal scattering cross sections in the libraries, which are summarized later, do not agree with the experimental data of Dilg *et al.* [27] of 3.761 ± 0.007 b, and

Mughabghab [28] adopted the same value with a slightly smaller uncertainty of 3.761 ± 0.006 b. In the modern evaluations, ENDF/B-VII.1, JEFF-3.1, CENDL-3.1, and ROSFOND have 3.852 b, and JENDL-4.0 has 3.841 b.

As Plompen [29], Hale, and Lubitz have noted, there appears to be a discrepancy between various data sets. Ohkubo (1984) and Johnson's (1974) measurements (above 1 keV) give a higher value compared with other measurements by Dilg, Koester, Block, and Melkonian. Lubitz has noted that discrepancies in various data sets could be related to the role of Doppler broadening of a constant cross section, which has not always been appreciated, and which gives a 3% effect for oyxgen at room temperature [30, 31]. Also, Plompen's weighted average of measurements of the coherent scattering length gives 5.825(1) fm, slightly higher than Atlas's 5.805(4) fm, but considerably smaller than the ENDF/B-VII.1 derived value of 5.875 - and Plompen and Lubitz note that these lower values for the coherent scattering length are consistent with a smaller total elastic cross section at low energies (5.825 fm gives a cross section of 3.787 b; 5.805 fm gives a cross section of 3.761 b) [29]. A high-accuracy measurement here would be most useful.

New R-matrix analyses that aim to resolve the differences are being performed by Hale and by Kunieda. These analyses, which include cross section and scattering length measurements, will correct measured data to 0 K values as needed, and bridge information that is contained in the higher energy and lower energy data. Kozier and Roubtsov [32] have noted this 3% discrepancy and that some heavy water criticality benchmarks seem to support a lower thermal scattering cross section (the impact on heavy water reactors is larger than on LWRs).

III. STRUCTURAL MATERIALS

A. ^{56}Fe

1. Summary of the evaluations

Although we saw a lot of "borrowing" from other evaluations in the ^{1}H and ^{16}O evaluations, the ^{56}Fe evaluations in the libraries are largely independent, with some exceptions such as the resolved resonance parameters. The evaluations rely heavily on the optical model and statistical model calculations, where the secondary particle energy and angular distributions play an important role in radiation shielding calculations.

The evaluations can be separated into four energy ranges: (a) the resolved resonance region up to 850 keV, (b) from 850 keV to about 7 MeV where fluctuation still persists in the measured total cross section, (c) from about 7 MeV to 20 MeV, and (d) above 20 MeV. The separation of regions (b) and (c) is only for the total and elastic scattering cross sections.

F. Perey and C. Perey of ORNL evaluated the resolved resonance parameters for ENDF/B-VI, and ENDF/B-VII.1 and CENDL have the same resonance parameter set. Other evaluations (JENDL, JEFF, and ROSFOND) adopt a modified version of the resolved resonances by Fröhner, performed for the JEF-2.2 evaluation.

In the MeV energy region, the fluctuation behavior seen in the experimental total cross sections, which an optical model cannot reproduce, should exist in the evaluated files, as this is crucial for neutron transport and shielding calculations. Usually the total cross sections in this energy region are obtained by tracing the experimental data available. For the other reaction channels, the Hauser-Feshbach model calculations are used for the evaluation, though the model codes employed are different.

As iron is one of the most important materials in experimental accelerator facilities, many evaluations go beyond 20 MeV. ENDF/B-VII.1 includes the LA-150 evaluation that goes up to 150 MeV, and JEFF-3.1 contains TALYS calculations all the way up to 200 MeV. Other files (JENDL-4.0, CENDL-3.1, and ROSFOND) just go up to 20 MeV, but JENDL-4.0 has a separate file for high energy applications (JENDL/HE).

2. Inelastic scattering

The nuclear data uncertainty assessment performed by WPEC Subgroup 26 for innovative reactor systems shows that the knowledge of the inelastic scattering cross section of ^{56}Fe should be improved to meet the target accuracy requirements for these systems. New measurements and evaluations have been requested in the range 0.5-20 MeV to reduce the uncertainty down to 2-10% depending on the energy region and the reactor considered (see the High Priority Request List at http://www.oecd-nea.org/dbdata/hprl/hprlview.pl?ID=454).

There are significant differences in evaluated inelastic scattering for iron. The difference in the inelastic scattering among the libraries mainly come from experimental data used. ENDF/B-VII.1, JENDL-4.0, and CENDL-3.1 include a resonance-like shape taken from experimental data up to 2.1 MeV. ROSFOND goes up to 5 MeV. JEFF-3.1 considers high-resolution experimental data, so that the fluctuation continues up to 10 MeV. Importantly, these differences are not only related to fluctuations that come from different experiments but there are significant differences in the multi-group averaged cross sections. This is evident by looking at the ratio of JENDL-3.3 and JEFF-3.1 to ENDF/B-VII.0 (= ENDF/B-VII.1) with the associated cross section uncertainties in a 40-energy group representation. Below 2 MeV the differences reach 28%. JENDL-3.3 and ENDF/B-VII.1 differ by only a few percent and agree within their uncertainties. However, there are significant discrepancies between these two evaluations and JEFF-3.1 below 5 MeV. JEFF-3.1 adopts small uncertainties. The original ENDF/B-VII.0 uncertainties between 1 and 2 MeV, which were about 3.3%, were increased to 16% in COMMARA-2 to

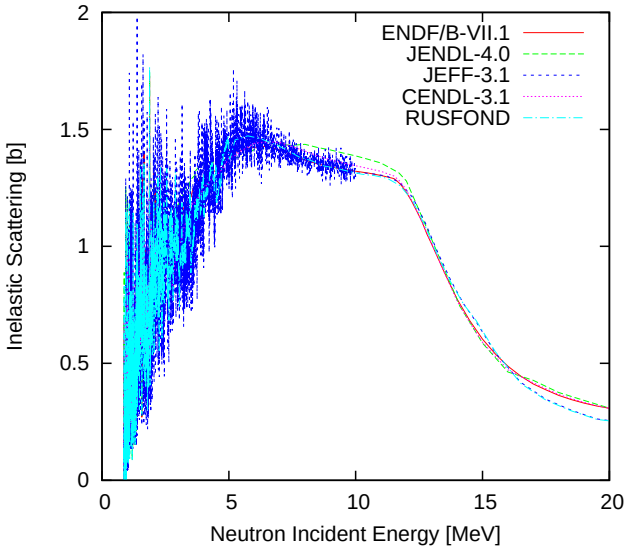

FIG. 3. Comparison of the evaluated inelastic scattering cross sections for ^{56}Fe.

reflect the large discrepancies between the various evaluations.

Above 10 MeV all libraries give a similar shape for the total inelastic scattering cross sections and the differences there are not so significant. For example, at 14 MeV they are 767 mb (CENDL), 774 mb (ENDF), 804 mb (JEFF), 773 mb (JENDL), and 800 mb (ROSFOND). The total inelastic scattering cross sections in these libraries are compared in Fig. 3.

Recent measurements by Wenner *et al.* [33] of neutron transmission through iron spheres at Ohio University, for quasi-monoenergetic neutrons ranging from ∼1 to ∼10 MeV, suggest a deficiency in the iron nonelastic cross section that progressively gets worse with increasing neutron energy. This was ascribed to deficiencies in the evaluated ENDF total inelastic cross section. The suggested reduction in the inelastic cross sections is large: the authors suggest decreases of 21%, 29%, and 35% at 6.2, 8.2, and 10.8 MeV respectively. At present ENDF/B-VII.1, JEFF-3.1, and JENDL-4.0 have similar total nonelastic cross sections in the 6–10-MeV range (approximately 1.4 b); Wenner *et al.* suggest that the correct value over this energy range decreases from about 1.1 b to 1.0 b, and they note that their model with Dietrich [34] (using insights from Wick's limit) supports such a reduced nonelastic cross section. Work is needed to study this question, and to apply optical model insights. These Ohio measurements confirm the ENDF/B-VII.1 total cross section to better than 1% in the 6 – 8 MeV range.

RPI has high-resolution transmission data up to 2 MeV, and scattering data ("quasi-differential data"), which need an MCNP calculation to compare with the data, for 0.5 to 20 MeV, and these point to improvements needed in ENDF for elastic and inelastic scattering. Nelson (LANL) has gamma-production data for iron. Plompen (Geel) has inelastic data from gamma-production measurements, measured recently from 800 keV to 5 MeV, that will also be valuable, and Schillebeeckx has made some new measurements. The analysis of these data, as well as SINBAD shielding benchmarks (EURACOS, ASPIS, IPPE, OKTAVIAN, *etc.*) is planned. Also, an OM is being developed by the IAEA for the analysis of iron scattering. To date, most evaluations use a spherical model but the soft rotor model proposed by Soukhovitskii [35] may be more appropriate, and the IAEA collaboration is seeking to develop a soft-rotor coupled-channels optical model that describes all scattering data. Such a model may also improve evaluated data representations of the unresolved resonance region. Finally, we note that the CEA is performing sensitivity studies to assess the importance of scattering angular distributions in the resonance region.

3. (n,xn) and (n,xp) reactions

The evaluated data for double-differential neutron or proton emission cross-sections in the 20–200 MeV range rely on pre-equilibrium models essentially constrained by proton-induced (p,xn) and (p,xp) experimental spectra. The lack of experimental data for double-differential (n,xn) spectra may introduce a bias in the model calculation predictions (see the High Priority Request List at http://www.oecd-nea.org/dbdata/hprl/hprlview.pl?ID=423.)

4. (n,α) reaction

There was a long-standing issue concerning the cluster emission in the pre-equilibrium process, where phenomenological alpha-particle knock-out models do not reproduce the recent measurements of alpha-particle productions at LANSCE/LANL. Since gas production in the structural material causes serious embrittlement problems in fusion reactors or other high energy applications, a better modeling of the cluster emission is crucial. This problem was addressed by applying an improved Iwamoto-Harada model [36], and the data files for these isotopes were upgraded by including Kunieda's new calculations. The new model also impacts the calculated alpha-particle energy spectra. ENDF/B-VII.1 includes these updates, and these high energy (n,α) cross sections were also incorporated into FENDL-3.0 at the IAEA.

IV. ACTINIDES

A. General comments

Before discussing each major actinide in turn, it is useful to address some general issues that apply to all the

existing actinide evaluations.

The major evaluated libraries (ENDF/B-VII.0, ENDF/B-VII.1, JENDL-4.0, JEFF-3.1 *etc.*) predict measured criticality extremely well (for many assemblies, but not all) when used in MCNP / TRIPOLI / MVP radiation transport simulations. This has been documented by many authors [1, 2, 4, 24, 37, 38], and most recently in a paper by van der Marck that compares these libraries for criticality applications [39]. However, such good performance in integral testing creates a false sense of optimism. In particular, a more careful look at the integral testing comparisons, and the fundamental and evaluated cross section data, points to various problems.

- **Compensating errors**
  Significant compensating errors must be present in most, and likely all, of the evaluations — see the next subsection for details.

- **Calibration**
  Calibration has been used in some cases in the evaluated databases to better match measured criticality of integral systems. Thus, agreement between simulated and measured criticality $k_{\rm eff}$ is not as impressive as it might seem, though of course a common set of evaluated data was used for all the neutronics simulations of *different* critical assemblies (that is, calibration was not done on an assembly-by-assembly basis!). Where some calibration was done it usually involved some reasonable physics assumptions and was not entirely ad hoc, and cross sections were usually adjusted within their uncertainty levels. Such a tiny calibration may also compensate some deficiencies in the data processing and transport calculations. The work by Iwamoto, described in the recent IAEA report [7], nicely shows (Fig. 4 in that report, p. 19) that fast neutron assembly uncertainties in calculated $k_{\rm eff}$, obtained by propagating the evaluated data covariances, are typically of the order of 1%, whilst the measured $k_{\rm eff}$ have uncertainties of about 0.1 – 0.2%, yet the calculations agree with the measured data (within the measured uncertainties for a high fraction of cases). This could only happen if some calibration has been done to better match the integral experiments.

- **Discrepancies**
  Plots of cross sections prepared by NNDC [17] clearly illustrate numerous discrepancies between the various evaluations. These discrepancies reflect both discrepancies amongst various measurements, and differences in theory, model parameters, and code calculations. The latter point has been documented in detail in the aforementioned IAEA report on actinide inelastic scattering and capture [7], where differences due to optical model formalisms and parameters were explored.

B. Compensating errors

An understanding has been established by the evaluation communities, and especially by Bauge *et al.* at the CEA [8], that the present fast neutron evaluations for ^{235,238}U, ^{239}Pu perform well in fast criticality simulations (Jezebel, Godiva *etc.*) — but for the wrong reasons! That is, they embody compensating errors between the roles of fission (cross sections, average number of prompt neutrons, and neutron spectra), capture, inelastic scattering and elastic scattering. A major challenge to our community is to strive to remove these compensating errors.

In fact, this situation has been recognized for a much longer period of time. The WPEC (Working Party on International Nuclear Data Evaluation Co-operation) was created in the late 1980s under OECD/NEA, and the summary notes from one of the first meetings [40] documented priority areas to tackle. In those notes, Kikuchi described the compensating effects of inelastic scattering and prompt fission neutron spectra on calculated criticality. This same point has been made more recently by Maslov, Ignatyuk *et al.* [41].

This topic was also discussed in detail in the IAEA report edited by Plompen *et al.* [7]. Quantitative advances have recently been developed by Romain of the CEA through the use of "Dalitz plots," a technique used in high energy physics. This approach quantifies the relative probabilities of three reaction mechanisms that comprise the total nonelastic cross section below the $(n, 2n)$ threshold — fission, inelastic, and capture — and facilitates a visual intercomparison of different evaluated cross section libraries. These plots indeed show that, especially for ^{239}Pu, ENDF/B-VII.1 and JEFF-3.1 differ significantly, yet both predict the criticality of $k_{\rm eff}$=1.000 accurately for Jezebel. For ^{238}U, though, the plot shows that differences between ENDF/B-VII.1, JENDL-4.0, and JEFF-3.1 are much smaller.

C. Fission cross sections

ENDF/B-VII.1, which has the same major actinide fission cross sections as ENDF/B-VII.0, uses the IAEA-WPEC-CSEWG standards as described by Carlson *et al.* [11], with some modifications to the unresolved resonance region. JEFF-3.1 and JENDL-4.0 use their own evaluation; in some cases there are differences with the standards values that lie outside the 1–σ uncertainties for the standards, and these discrepancies should be resolved.

D. Prompt fission neutron spectra

Although the PFNS (prompt fission neutron spectrum) for major actinides in ENDF, JEFF, and JENDL are not identical, they tend to be rather similar as they all trace their origins to the Madland-Nix Los Alamos

model. ENDF/B-VII.1 contains the updated Madland-Nix model evaluated for ENDF/B-VII.0 [37]. The PFNS data in JENDL-4.0 below 5 MeV are identical to those in JENDL-3.3, evaluated by Ohsawa *et al.* [42], and CCONE calculations were adopted above 5 MeV. In JEFF-3.1, the PFNS of ^{235}U is the same as in ENDF/B-VI, and new Madland-Nix-type model calculations performed by Vladuca and Tudora [43] were adopted for ^{238}U and ^{239}Pu.

Major efforts are underway to advance our understanding of PFNS. These involve the "Chi-nu" measurement capabilities being developed by LANL, LLNL, and the CEA at LANSCE, theoretical development at many places, and a wide body of work coordinated by an IAEA CRP [44].

Most recent evaluations of ^{239}Pu PFNS are based on the Madland-Nix model in its original or some revised version that takes into account more parameters to better fit detailed prompt neutron data, *e.g.*, different neutron multiplicities from light and heavy fragments, different temperatures in the two fragments, anisotropy of emission of the neutrons, *etc.* At higher energies, JENDL-4.0 includes pre-equilibrium components of the spectrum. Significant experimental and theoretical efforts are underway to shed some light on the low- and high-energy tails of the n+^{239}Pu PFNS, which should help resolve some of the remaining uncertainties.

Issues to be solved include the following.

- Does the shape of the PFNS need to be higher below an MeV (say 10% higher near 0.1 MeV outgoing neutron energy) for essentially all incident energies and all actinides, as suggested by some experimental data sets and by Maslov? At the present time this remains an open question, needing more experimental work (to ensure that erroneous multiple-scattering backgrounds are not biasing the data) and more theoretical analyses.

- If the above proposal is adopted, this will impact thermal system ^{235}U and ^{239}Pu criticality (*e.g.*, the average energy of ^{235}U PFNS at thermal might decrease from 2.03 to 1.99 MeV). Can good thermal criticality performance be re-established via other nuclear data changes?

- Dosimetry threshold data in fast LANL critical assemblies (Jezebel and Pu-Flattop; Godiva and Flattop-25) may provide guidance on the shape of the high emission energy PFNS for fast incident energies [45] (see later in this paper, Figs. 5, 7). Additional work is needed to quantify the uncertainties in this analysis.

- Are we confident that Zolotarev's [46] evaluations of dosimetry cross section activations in ^{235}U PFNS at thermal energy, and ^{252}Cf spontaneous fission neutron spectra, point to the correctness from 1 to 10 MeV outgoing neutron energies of the existing ENDF/B-VII.1 evaluations? Initial discussions suggest that the Cf results might be reliable, but that larger uncertainties may be present in the thermal uranium dosimetry analysis owing to the extent to which the uranium plate in the experiment truly creates a thermal PFNS spectrum. Work beginning on a new IAEA CRP for validation of dosimetry data will help resolve this.

- LANL released data for NUEX measured PFNS appear to corroborate ENDF/B-VII PFNS data for ^{235}U and ^{239}Pu from about 1 to 7 MeV outgoing energies, for fast neutron incident energies [1, 47] (see later in this paper, Figs. 5, 7). Are the very small uncertainties quoted reliable?

- How do neutrons from multi-chance fission change the PFNS shape? Kawano *et al.* [48] incorporated the FKK theory into the prompt fission neutron spectrum calculations, and the CCONE calculations in JENDL-4.0 combine the pre-equilibrium process with the Los Alamos model [49] where the multi-chance fission occurs. Owing to the pre-equilibrium emission, the PFNS at higher energies is anisotropic. In general, refined theoretical treatments are needed to describe experimental PFNS above the second-chance emission threshold for actinides.

E. Prompt fission gamma-ray spectra

Evaluated prompt fission gamma-ray spectra (PFGS) tend to be based on very old measurements, and updates are needed to reflect new measurements, including those made recently at LANSCE/DANCE. New reactor design work has identified uncertainty requirements of 7.5% for gamma-ray heating in peripheral non-fueled zones, yet current discrepancies in C/E for integral benchmarks can be as high as 10-28% (see High Priority Request List http://www.oecd-nea.org/dbdata/hprl/hprlview.pl?ID=422 (and 421)). New evaluations should be based on all available experimental information, as well as on model calculations such as CGMF (Los Alamos) [50–52] , FREYA (LLNL-LBNL) [53, 54], and GEF (Schmidt) [55].

F. Inelastic scattering

There are very significant differences amongst the various evaluations. For example, for the total inelastic scattering cross section of ^{239}Pu, ENDF/B-VII.1 and JENDL-4.0 are close in the 0.5–3 MeV region. However JEFF-3.1 is significantly lower. For ^{238}U, the various evaluations are reasonably close between 0.7 and 3 MeV. However ENDF/B-VII.1 is notably higher in the 0.2–0.6 MeV range (see the useful review by Plompen *et al.* [7]).

Since inelastic scattering to the low-lying states of actinides is very difficult to separate experimentally from

elastic scattering, the evaluation of inelastic scattering cross sections relies on model calculations, where many uncertain factors are involved, such as the optical potential parameters, nuclear deformation, width fluctuation corrections, fission competition, *etc.* It is essential to understand differences in the statistical model calculations and the model parameters adopted by various groups. Differences in partitioning the total incoming flux into the elastic and inelastic channels may also change the scattering angular distributions.

Discrepancies exist between evaluated and measured 14 MeV incident neutron double-differential neutron emission data [56, 57] for ^{238}U, especially for neutron energies above 10 MeV where a significant underestimation is seen near $Q = -2$ MeV. One might attribute this to unknown collective strength that increases the inelastic scattering to continuum states, and it was handled in ENDF/B-VII.0 [58] and JEFF-3.1 using an empirical approach with pseudo-levels to represent data. Insights were obtained not only from Baba's ^{238}U data [56, 57] but also from similar ^{235,238}U data from Kammerdiener [59], and from analyzing LLNL 14 MeV pulsed sphere measurements [45]. The pseudo-level was also adopted in JENDL-3.2 by Kawano *et al.* [60] in order to better fit such data. However, these pseudo-levels were removed in JENDL-3.3 [61] as they are less justifiable from a fundamental theoretical view. A recent MSD (multi-step direct) calculation based on the quasi-particle random phase approximation by Dupuis *et al.* [62] reproduced the spectra at 90° and 120° without any adjustable parameters, although disagreement still remains at 30°. Also, a MSD treatment by Wienke *et al.* [63] emphasizing the importance of deformations and the collective structure of actinide targets provides an alternative approach. Ongoing work at Livermore is also focused on the theoretical understanding of such processes through the calculation of transition densities to QRPA excited states.

Since neutron transport properties (such as room returns, multiple scattering, *etc.*), as well as the underlying cross sections, are required to model neutron transmission measurements, a better modeling of the experiments is also essential to resolve this problem [64]. In addition, PFNS representations that contain a pre-equilibrium prefission angular component that is anisotropic should be implemented in all evaluations.

G. Radiative capture

In general it is difficult to measure capture cross sections for fissile actinides, owing to the difficulty in separating the capture gamma-rays from the prompt fission gamma-rays, though recent progress has been made at LANSCE (LANL), Rensselaer (RPI), and n-TOF (CERN) to solve this difficulty. The activation method avoids this difficulty, but typically this is only possible for limited incident energies (*e.g.* thermal) and quasi-monoenergetic neutron sources. The capture cross section can sometimes be inferred reliably from simultaneous fits to the total and partial cross sections.

H. ^{235}U

1. *Resolved resonance parameters*

All the existing libraries adopted the resolved resonance parameters for ^{235}U from ORNL [65]. The upper energy boundary of the resolved region, which is 2.25 keV, was lowered to 500 eV in JENDL-4.0 and point-wise cross sections are provided in the 500 eV to 2.25 keV energy range based on the previous resolved resonance parameter set from ORNL [66]. Hence the cross sections below 500 eV in all the libraries are identical. New work on ^{235}U is needed to solve a number of open problems, as discussed below (see also the High Priority Request List at http://www.oecd-nea.org/dbdata/hprl/hprlview.pl?ID=430).

2. *Radiative capture*

The capture cross section in the resolved resonance region is given by the resonance parameters from ORNL [65]. In the fast energy range, although unresolved resonance parameters were also provided by ORNL, the evaluations are based on available experimental data. The evaluation in ENDF/B-VII.1 is based on an analysis of measured capture and α-value (capture to fission ratio) data above 2.25 keV. ROSFOND adopted ENDF/B-VII.1. JEFF-3.1 adopted ENDF/B-VI.8, which resulted in very similar cross sections above 25 keV.

Questions associated with the ^{235}U capture cross section should be resolved, especially in the 0.5–2 keV energy range where the recent JENDL-4.0 evaluation lowered the cross section by more than 25% based on integral reactor (sodium void) testing [67]. Also, their analysis led to increased capture compared to ENDF and JEFF in the 3–5 keV region, and for 100–1000 keV. New data from LANSCE (LANL) by Jandel *et al.* [68] with the DANCE detector partly support the Japanese conjecture (from 1 to 5 keV), but also suggest that a ∼10% capture increase is needed from 10 to 70 keV for all evaluations, as shown in Fig. 4. Recent measurements by Danon *et al.* at RPI also support a lower capture cross section in the 100 eV –2 keV region.

Other more integral measurements of capture also point to work needed to resolve discrepancies. Measured PROFIL [69] fast reactor measurements of ^{235}U capture are 3–5% above MCNP simulations that use the ENDF/B-VII.1 capture cross sections [24]. Yet the recent accelerator mass spectrometry data by Wallner *et al.* would instead suggest the capture data in ENDF/B-VII.1 should be 5–8% *lower* at 25 keV and 423 keV [1].

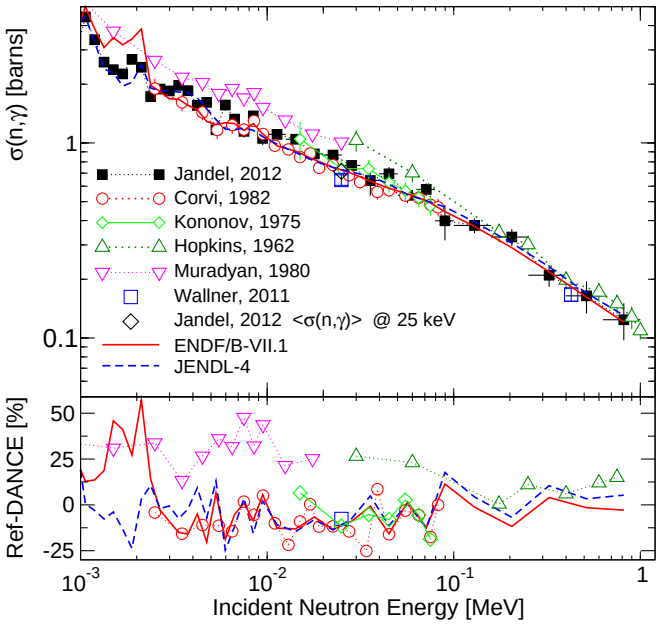

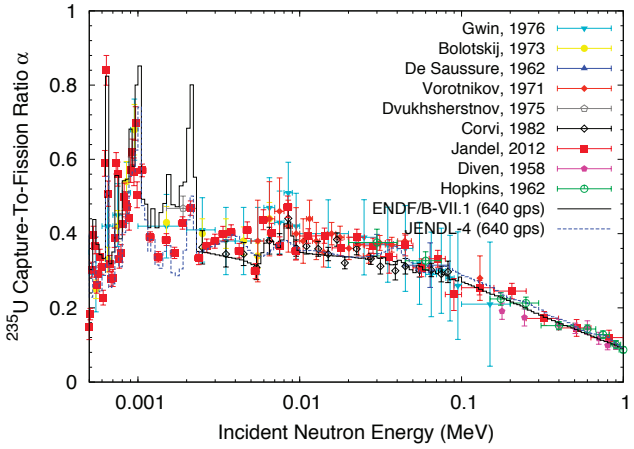

FIG. 4. ^{235}U capture (upper-panel) and alpha (capture to fission ratio, lower panel), showing recent LANL (DANCE) measurements by Jandel *et al.*

3. *Inelastic scattering*

From threshold to a few MeV there are significant differences between JENDL-4 and ENDF/B-VII.1 (JEFF-3.1 is the same as ENDF/B-VI) up to 50 keV, exhibiting differences in the treatment of the low-lying rotational band built upon the isomeric state. All evaluations lie significantly higher than some of the measurements in the 1–2 MeV range (but we note that the direct measurement of total inelastic scattering has a large uncertainty). ROSFOND takes ENDF/B-VII.1, with some modifications to individual levels. JENDL-4.0's independent analysis appears similar to ENDF/B-VII.1 from 50 keV up to a few MeV, but then differences are seen at higher energies. These differences have a large impact on the fast criticality (Godiva), leading to a 540 pcm swing in calculated criticality, as shown by Go Chiba [71]. Differences exist not only in the total inelastic cross section but also in the partial cross sections to individual levels and their angular distributions. Experts in coupled channel and Hauser-Feshbach calculations need to resolve these differences.

We note that MacFarlane has suggested that the inelastic scattering for incident energies ∼0–4 MeV in ^{235}U might need to be smaller, based on the systematic under-calculation (by a few percent) of spectral indices ^{238}U fission/^{235}U fission (fission ratio) in Godiva and Flattop-25 — less inelastic scattering would lead to a hotter neutron spectrum in the assembly, and consequently a higher ^{238}U fission/^{235}U fission ratio. This needs to be studied, along with the role of the PFNS shape on such spectral indices.

4. *(n,2n) reaction*

ENDF/B-VII.1, JEFF-3.1 (same as ENDF/B-VI), and JENDL-4.0 are in fair agreement, and are consistent with data of Frehaut [72], as well as the measurements from Younes *et al.* using the GEANIE detector at LANSCE together with model calculation extrapolations. Note that CEA reported a normalization factor that should be applied to the data of Frehaut for all Gd-tank measurements of $\overline{\nu}$, $(n, 2n)$ and $(n, 3n)$, and Vonach suggested a value of 1.078 for this normalization [73].

5. *Average number of neutrons per fission $\overline{\nu}$*

A common method of evaluating $\overline{\nu}$ is a direct fitting of a simple functional form to experimental data available, taking into account uncertainties associated with the data. The ENDF/B-VII.1 $\overline{\nu}$ evaluation comes from a covariance analysis of the measured data, though in the fast region the evaluation was modified slightly (within the uncertainties) to optimize a match to the fast critical assembly benchmarks [58]. The evaluations of prompt and total fission multiplicity, $\overline{\nu}_p$, $\overline{\nu}_t = \overline{\nu}_p + \overline{\nu}_d$, appear to be very similar, although JENDL-4.0 lies under ENDF/B-VII.1 in the 10–15 MeV region, probably due to the energy grid given in the file (JENDL-4.0 gives only five energy points above 5 MeV, whilst the ENDF/B-VII.1 energy grid is denser).

The total thermal $\overline{\nu}$ value in ENDF/B-VII.1 (2.4367) differs slightly from the evaluated constant by the standards group (2.4355) owing to the calibration to thermal reactor benchmarks. JENDL-4.0 has a very similar value (2.4363) which is based on the experimental data of Gwin *et al.* [75, 76].

6. *PFNS integral validation*

Los Alamos has been exploring the use of dosimetry $(n, 2n)$ detectors in fast critical assemblies to provide

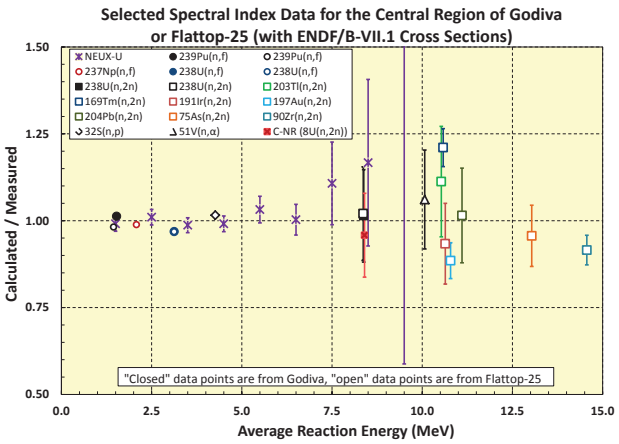

FIG. 5. Integral validation testing of dosimetry threshold reactions in uranium fast critical assemblies, providing a test of the ^{235}U prompt fission neutron spectrum for higher neutron emission energies. The x-axis shows the average incident neutron energy at which the reaction occurs. Deviations from C/E=1 could point to $(n, 2n)$ cross section deficiencies as well as PFNS deficiencies. The uncertainties shown include both measurement uncertainties and calculation uncertainties from the evaluated cross sections but do not include uncertainties in the evaluated PFNS spectrum. Numerical values for the data and calculations are given in Table I. Uranium NUEX PFNS data that have been recently released by Los Alamos are also shown [47].

insights into the shape of the high-energy prompt fission neutron spectrum. The MCNP code can simulate the neutron transport in fast assemblies, such as Jezebel (a Pu sphere), Flattop-25, and Flattop-Pu (spheres of ^{235}U and ^{239}Pu surrounded by a ^{238}U tamper), using ENDF/B-VII.1 cross sections. We expect the MCNP-predicted high energy neutron spectrum above a few MeV to be highly dependent on the shape of the underlying PFNS in the ENDF/B-VII.1 database. Discrepancies between predictions and measurements of the dosimetry $(n, 2n)$ rates point to possible deficiencies in the evaluated PFNS. By using activation cross sections from $(n, 2n)$ dosimetry detectors to characterize the high-energy spectrum, we can seek to validate the evaluated PFNS. This approach depends upon having accurate $(n, 2n)$ cross sections for the dosimetry reactions, and therefore (a) we use dosimetry materials for whose $(n, 2n)$ cross sections have been measured by many groups and have relatively small uncertainties and (b) we use as many detectors as we can so that individual detector $(n, 2n)$ cross section biases are likely to cancel out.

The appendix summarizes the historical Los Alamos fast critical assembly measurements that we use for this analysis, and relevant averages of these data (where multiple measurements were made) are presented in Table I along with our MCNP5 calculations. These measured

TABLE I. Calculated and measured reaction rates (in ratio to ^{235}U(n, f)) for various threshold reactions in the central region of fast Los Alamos critical assemblies. The data for the uranium-235 assemblies (Godiva and Flattop-25) are presented in Fig. 5, whereas data for the ^{239}Pu assemblies (Jezebel and Flattop-Pu) are presented in Fig. 7. See the Appendix for more details on these data. Calculations come from MCNP5 simulations using ENDF/B-VII.1 data, and include cross section uncertainties where available, but not contributions from the PFNS spectra uncertainties. The measured data given are averages of multiple measurements if more than one exist, and uncertainties include a random component obtained from replicate experiments (3%) and a systematic component that comes from the 14.1 MeV cross section uncertainty in the calibration process (see text and Table IV).

Assembly/ Reaction	**Calculation**	**Experiment**
GODIVA		
^{238}U$(n, 2n)$	7.84E-3 ± 13%	7.73E-3 ± 4%
Flattop-25		
^{238}U$(n, 2n)$	7.08E-3 ± 13%	6.94E-3 ± 4%
^{203}Tl$(n, 2n)$	1.70E-3 ± 13%	1.52E-3 ± 6%
^{169}Tm$(n, 2n)$	1.78E-3 ± 3%	1.47E-3 ± 4%
^{191}Ir$(n, 2n)$	1.76E-3 ± 12%	1.89E-3 ± 4%
^{197}Au$(n, 2n)$	1.43E-3 ± 5%	1.61E-3 ± 3%
^{204}Pb$(n, 2n)$	1.66E-5 ± 12%	1.64E-5 ± 6%
^{75}As$(n, 2n)$	1.43E-4 ± 7%	1.50E-4 ± 6%
^{90}Zr$(n, 2n)$	4.40E-5 ± 3%	4.85E-5 ± 3%
^{32}S(n, p)	3.11E-2	3.06E-2 ± 6%
^{51}V(n, α)	1.18E-5 ± 12%	1.11E-5 ± 6%
Jezebel		
^{238}U$(n, 2n)$	1.32E-2 ± 12%	1.06E-2 ± 4%
^{169}Tm$(n, 2n)$	3.72E-3 ± 3%	3.13E-3 ± 3%
^{191}Ir$(n, 2n)$	3.76E-3 ± 11%	3.21E-3 ± 4%
Flattop-Pu		
^{238}U$(n, 2n)$	1.10E-2 ± 12%	9.02E-3 ± 4%
^{203}Tl$(n, 2n)$	2.92E-3 ± 13%	2.27E-3 ± 6%
^{169}Tm$(n, 2n)$	3.05E-3 ± 3%	2.43E-3 ± 3%
^{191}Ir$(n, 2n)$	3.08E-3 ± 11%	2.83E-3 ± 4%

data have been reassessed and updated to modern calibration standards. Fig. 5 shows our results for uranium critical systems. The $(n, 2n)$ and (n, f) reactions are most sensitive to the ^{235}U nuclear data, with the $(n, 2n)$ reactions being particularly sensitive to the PFNS. Although there are some inconsistencies between the feedback from the different detectors, especially from Zr and Tm, overall the validation comparisons shown in Fig. 5 indicate that the high-energy PFNS spectrum (for fast incident neutrons) appears to be reasonable, and there is no clear indication that the high-energy tail should be higher or lower. We note that this conclusion differs from our earlier results which were based on a smaller number of detectors, and on dosimetry activation data before the calibration basis was updated (our earlier studies [45] suggested the need for a softer ^{235}U PFNS above 8 MeV

for fast incident neutrons). The principal change is that our ^{191}Ir$(n,2n)$ measured data has been reassessed to be larger than before (see Appendix). Our present conclusion also appears to differ from preliminary CEA results [77] which had also suggested the need for a softer ^{235}U PFNS, from dosimetry feedback from a fast critical assembly in France. Future work is needed to understand the LANL and the CEA different results, and indeed a new IAEA CRP on dosimetry data validation will address this subject.

Later, in Section IV J 6, we provide analogous information on testing the ^{239}Pu PFNS for fast incident neutrons.

I. ^{238}U

1. Radiative capture

The resolved resonance parameters evaluated by ORNL and the CEA [78] are given up to 20 keV in ENDF/B-VII.1, JEFF-3.1, JENDL-4.0, and ROSFOND. CENDL-3.1 adopted the resonance parameters in JENDL-3.3. Above the resolved resonance region, there is now better consensus amongst the various libraries, together with consistency with the IAEA-WPEC-CSEWG standards result. The evaluated uncertainties are rather small — 2% in some cases in the fast energy range. The recent AMS data by Wallner *et al.* at 25 and 426 keV support these evaluations (see Ref. [1] p. 2970).

The international communities' success in determining this important cross section accurately, through both WPEC Subgroup 4, 22 and through the IAEA-WPEC-CSEWG standards effort, is one of the notable accomplishments in recent decades. However, there is one issue that needs to be resolved. The ENDF/B-VII evaluation made some small modifications to the standards capture result: for example, in the 20 – 100 keV region, a value that is a few percent above the standards value was adopted, motivated by the *shape* predicted by GNASH model calculations [70] as well as by improved MCNP simulation performance for the Bigten critical assembly. But as this small modification exceeded the uncertainties of the standards evaluation, future work is needed to resolve these differences. Moreover, the nuclear data uncertainty assessment performed by WPEC Subgroup 26 for innovative reactor systems shows that the uncertainty in the radiative capture cross section of ^{238}U should be further reduced to 1-3% in the energy range from 20 eV to 25 keV (see High Priority Request List at http://www.oecd-nea.org/dbdata/hprl/hprlview.pl?ID=456). The recent ENDF/B-VII.1 evaluation of this cross section uncertainty (3-4% in this energy range) suggests that additional measurements in the resonance regions are still needed. Indeed, new measurements are being planned by Cano Ott *et al.* in Europe, at the CERN n_TOF facility and at IRMM GELINA, with the goal of further improving our understanding of the ^{238}U capture cross section from a few eV to several hundred keV [7].

2. Elastic and inelastic scattering

As was the case for ^{235}U, there are significant differences between the different cross section libraries, both for elastic and inelastic cross sections and for angular distributions. Cross section differences are evident in the total inelastic as well as in the partial cross sections to individual levels. This can lead to significant impacts on calculated criticality [71] for fast systems. Indeed, feedback from integral reactor sensitivity studies in the USA, Japan, Europe, and WPEC Subgroup 26, 33 have consistently pointed to the need for more accurate ^{238}U inelastic cross sections and angular distributions [79–82] (see also High Priority Request List at http://www.oecd-nea.org/dbdata/hprl/hprlview.pl?ID=435).

Recent "quasi-differential" measurements from RPI that are sensitive to elastic and inelastic scattering in ^{238}U provide useful guidance on how to improve the scattering cross sections. These data are from 0.5 up to 20 MeV incident energies. ENDF/B-VII does not include anisotropic angular distributions in compound elastic scattering (JENDL has this and does better at backward angles). At forward angles the libraries perform better than at backward-angles, where clear deficiencies can be seen. For ENDF/B-VII the problem seems to be in its angular distribution representations, while for JEFF-3.1 the problem seems to be in its cross sections (JEFF-3.1 has an anisotropic elastic compound component). Also, ENDF/B-VI appears to perform better than ENDF/B-VII.1. The VII.1 (=VII.0) results were based on a pragmatic choice a decade ago by Young, MacFarlane and Chadwick, using Maslov's optical model that led to good performance in critical assembly simulations, but improvements may now be needed. The IAEA has ongoing work (Capote, Trkov) on calculations and benchmarks based on a new dispersive coupled-channel potential that couples almost all levels below 1 MeV. A developmental test evaluated file has already been made and tested with encouraging results against a suite of twelve ICSBEP benchmarks that are especially sensitive to elastic scattering. Work at Livermore and Los Alamos on coupled-channel scattering for the actinides will also be relevant to this project, as Thompson, Dietrich, and Kawano showed that great care is needed to ensure that convergence is achieved in the scattering calculation.

3. $(n,2n)$ reaction

There is fair agreement among the libraries, although ENDF/B-VII.1 rises from a threshold about 10% higher than JENDL-4.0 in the 7–9 MeV region. This was motivated in ENDF by a desire to match the LANL Knight data [83]. Most data appear to lie below Knight though the data of Kornilov *et al.* [84] are also higher in the threshold region and close to ENDF/B-VII.1. It will be important to resolve such $(n,2n)$ threshold discrepancies, because the ^{238}U$(n,2n)$ reaction is used as a dosimetry

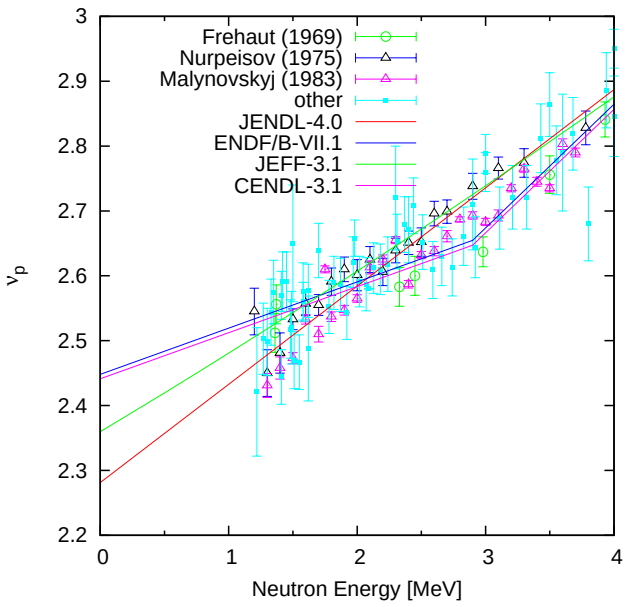

FIG. 6. Comparison of the evaluated $\overline{\nu}_p$ for ^{238}U with experimental data.

reaction in assessments of the higher-energy tail of the prompt fission spectrum, a topic of current intense study.

Recent $(n, 2n)$ measurements by Zhu *et al.* [85] agree well with ENDF/B-VII.1. For example, the experimental value at 14.1 MeV is 858 ± 34 mb, which confirms the ENDF value at 14.1 MeV of 849 mb, while CENDL-3.1 has 871 mb, JEFF-3.1 has 849 mb, and JENDL-4.0 has 943 mb.

4. *Average number of neutrons per fission* $\overline{\nu}$

There appear to be some significant differences in the evaluations below 4 MeV that should be resolved. As seen in Fig. 6, ENDF/B-VII.1 and CENDL-3.1 have a kink at 2.9 MeV, while JENDL-4.0 and JEFF-3.1 have a linear extrapolation toward zero energy. These representations coincide at 2 MeV but large differences are evident at 3 MeV. Since the average neutron energy causing fission in ^{238}U in critical assemblies such as Bigten is about 3 MeV (owing to the $\sim$ 1 MeV fission threshold), as shown in the Appendix of Selby's paper [86], this discrepancy impacts criticality calculations and should be resolved.

The linear interpolation toward zero energy defined in ENDF/B-VII.1 results in too high a value for $\overline{\nu}$ at the thermal energy. This was also supported by the Madland-Nix model calculation, which gives lower $\overline{\nu}$, similar to JENDL-4.0 and JEFF-3.1 values. But because the ^{238}U fission cross section at thermal energies is of the order of μb, this does not have an impact on practical calculations.

J. ^{239}Pu

1. *Resolved resonance parameters*

Derrien *et al.* of ORNL performed resolved resonance analysis in the energy range 0 – 2.5 keV [87]. JENDL-4.0 adopted these same resonance parameters. JEFF-3.1.1 includes some modifications to these resolved resonances for a better match to some integral $k_{\rm eff}$ data. These modification were motivated by the problem of an over-prediction of calculated $k_{\rm eff}$ in ^{239}Pu solution critical assemblies [1, 24] (see also the High Priority Request List and references therein at http://www.oecd-nea.org/dbdata/hprl/hprlview.pl?ID=427). WPEC Subgroup 34 "Coordinated evaluation of ^{239}Pu in the resonance region" was formed to help address these issues. As an example of the magnitude of this problem, in reflected critical assemblies with high concentrations of ^{239}Pu within a thermal neutron spectrum (*e.g.* some of the PU-SOL-THERM benchmarks) there is an overall trend in C/E of $k_{\rm eff}$ of 1.005 – 1.01, using ENDF/B-VII.1 (=VII.0) data [24].

An improved modeling of plutonium solution critical assemblies is likely dependent not only upon resonance parameter analyses but also on the values for $\overline{\nu}$ and the PFNS shape, as reported by Subgroup 34. The goal for Subgroup 34 is to improve our modeling of such integrated criticality experiments whilst advancing the understanding, and evaluation, of the underlying nuclear data.

It is also possible that angular distributions from resonance fission neutrons are needed for high-fidelity simulations of criticality.

2. *Radiative capture*

The nuclear data uncertainty assessment performed by WPEC Subgroup 26 for innovative reactor systems shows that the knowledge of the radiative capture cross section of ^{239}Pu should be improved to meet the target accuracy requirements for these systems. New measurements and evaluations have been requested from 2 keV up to about 1.5 MeV to reduce the uncertainty down to 3-7% depending on the energy region and the reactor considered (see the High Priority Request List at http://www.oecd-nea.org/dbdata/hprl/hprlview.pl?ID=451).

There are significant (on the order of 10%) differences amongst the evaluations in the fast region, and above 0.6 MeV ENDF/B-VII.1 falls well below the Los Alamos data of Hopkins and Diven [88]. PROFIL [69] fast reactor data analyses suggest ENDF/B-VII.1 may be on average 10% too low in the fast region, while JEFF-3.1 performs better here. These PROFIL data may be the only integral data on ^{239}Pu capture in the fast range as neither Los Alamos nor Japan (we understand) have their own integral measurements (such measurements can be difficult owing to the ingoing ^{240}Pu often present in ^{239}Pu

samples). It is striking that in the important 200 keV - 1 MeV region there is only one measurement, that of Hopkins and Diven from Los Alamos from the early 1960s! ENDF/B in particular needs to be updated. Future Los Alamos DANCE experiments that build on the recent detector advances made for ^{235}U capture hope to better determine the cross section. These experiments should also strive to reach higher accuracies in the hundreds of keV region as well as at lower energies.

Also, nuclear reaction theory is especially important for evaluating the capture cross section because we have so little data above 100 keV. Such calculations must treat the fission competition channel, and associated channel width fluctuations, accurately. The role of (n,γf) processes need to be carefully considered.

3. *Inelastic scattering*

As discussed earlier [7], there are significant differences amongst the evaluations for ^{239}Pu in the fast energy range, with ENDF/B-VII.1 and JENDL-4.0 lying significantly above the JEFF-3.1 evaluation. Data reported by Batchelor and Wyld [89] and Andreev [90] suggest a smaller total inelastic scattering for ^{239}Pu, although these data were not measured directly. Maslov and Ignatyuk have also suggested that ENDF/B-VII.1 and JENDL-4.0 inelastic scattering cross sections in the fast range are too large, and they postulate that they compensate an ENDF/B-VII.1 PFNS spectrum that is too low below 1 MeV. Ideally, new accurate measurements would be performed to better determine inelastic scattering, but we are not aware of any immediate prospects for this. Work is needed by experts in coupled channels and Hauser-Feshbach reaction theory to better understand plutonium scattering reactions.

4. $(n, 2n)$ *reaction*

ENDF/B-VII.1 and JENDL-4.0 are in fair agreement, and match the GEANIE data [91] and the activation data of Lougheed *et al.* [92] near 14 MeV. JEFF-3.1 rises more rapidly from threshold, and lies below the data of Lougheed *et al.* at 14 MeV [92]. PROFIL measurements [69] tend to suggest a smaller $(n, 2n)$ cross section, at least in its rise from threshold [24]. However, other integral measurements support the ENDF/B-VII.1 ^{239}Pu$(n, 2n)$ evaluation as shown in Fig. 7 (the larger error bar on the ^{239}Pu$(n, 2n)$ data point in the figure comes from our large uncertainty in the evaluated $(n, 2n)$ cross section near its threshold, not measurement uncertainties).

5. *Average number of neutrons per fission* $\overline{\nu}$

Independent statistical analyses were performed for ENDF/B-VII.1, JEFF-3.1, and JENDL-4.0. CENDL-3.1 adopted the data in JENDL-3.3, and ROSFOND took the JEFF-3.1 file. ENDF/B-VII.1 applied a small modification to match Jezebel $k_{\rm eff}$. In one region the tweak lay outside the 1-σ error bar. This tweak should be removed in the future. Also, recent work by WPEC Subgroup 34 may lead to an updated recommendation on the ^{239}Pu $\overline{\nu}$ at lower energies.

The total thermal $\overline{\nu}$ value in ENDF/B-VII.1 (2.879) differs slightly from the evaluated constant by the standards group (2.884 $\pm$ 0.16%) [37]. JEFF-3.1, and ROSFOND have 2.8778 (ROSFOND is the same as JEFF-3.1), JENDL-4.0 has 2.8786, and CENDL-3.1 adopted the JENDL-3.3 value, which is 2.8843. Given the well-known over-prediction of $k_{\rm eff}$ in thermal plutonium critical assemblies, there is a need to study the limits of how low an evaluated thermal $\overline{\nu}$ could be. The evaluated values in ENDF/B-VII.1, JEFF-3.1, and JENDL-4.0 are already 1-σ below the standards evaluation. Does the standards constant need re-evaluating? We note that the optimized search approach by Rochman and Koning [93] was able to match thermal solution Pu criticality better, albeit at the cost of using a thermal $\overline{\nu}$ value that is 0.3% below ENDF/B-VII.1, which is 3 standard deviations below the standard.

6. *PFNS integral validation*

See Section IV H 6 for a summary of our work to test the PFNS using Los Alamos fast critical assemblies. Here we provide our results for the ^{239}Pu PFNS based on historical dosimetry activation measurements made in Jezebel and Flattop-Pu.

We expect the MCNP-predicted high-energy neutron spectrum above a few MeV to be highly dependent on the shape of the underlying PFNS in the ENDF/B-VII.1 database; likewise, discrepancies between predictions and measurements of the high energy spectrum point to possible deficiencies in the evaluated PFNS.

The appendix summarizes the historical Los Alamos fast critical assembly measurements that we use for this analysis, and relevant averages of these data (where multiple measurements were made) are presented in Table I along with our MCNP5 calculations. These data have been reassessed and updated to be based on modern calibration standards. Fig. 7 shows our results for plutonium fast critical systems. The $(n, 2n)$ and (n, f) reactions are most sensitive to the ^{239}Pu nuclear data, with the $(n, 2n)$ reactions being particularly sensitive to the PFNS. These data suggest that for outgoing neutron energies above 10 MeV the ENDF/B-VII.1 ^{239}Pu PFNS may need to be softer, as we suggested in Ref. [45]. Therefore, unlike the case for ^{235}U PFNS discussed in Section IV H 6, the process of updating our dosimetry measured values and adding additional materials (thallium in this case) has not changed our earlier conclusions. But this kind of dosimetry testing for the PFNS should still be treated cautiously because we have fewer data for plutonium assemblies than

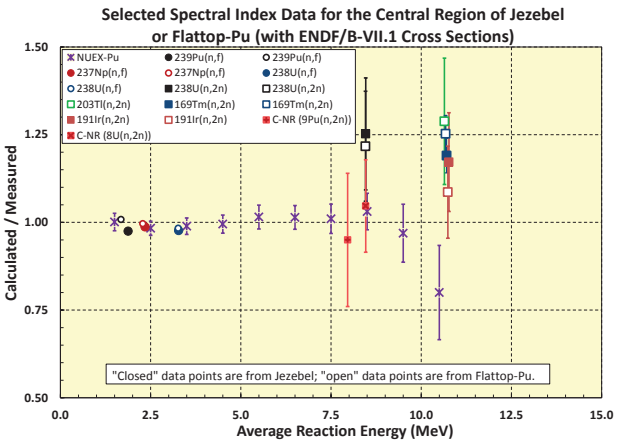

FIG. 7. Integral validation testing of dosimetry threshold reactions in plutonium fast critical assemblies, providing a test of the ^{239}Pu prompt fission neutron spectrum at higher neutron emission energies. The x-axis shows the average incident neutron energy at which the reaction occurs. Deviations from C/E=1 could point to $(n, 2n)$ cross section deficiencies as well as PFNS deficiencies. The uncertainties shown include both measurement uncertainties and calculation uncertainties from the evaluated cross sections but do not include uncertainties in the evaluated PFNS spectrum. Numerical values for the data and calculations are given in Table I. Plutonium NUEX PFNS data that have been recently released by Los Alamos are also shown [47].

for uranium assemblies and it is possible that the overcalculation in Fig. 7 is instead due to $(n, 2n)$ cross section deficiencies rather than to PFNS deficiencies. Indeed, the NUEX data shown in the figure appear to be in conflict with the dosimetry data, and instead support the existing ENDF/B-VII PFNS evaluation up to 10 MeV. Again, a new IAEA CRP on dosimetry data validation will address this subject.

V. VALIDATION BENCHMARKS

The CIELO project will pay close attention to integral validation testing of the new evaluations, with the goal of creating a suite of new evaluated files that perform very well in simulations of an agreed set of validation experiments. Our goal is for validation comparisons that are as good, and hopefully better, than the current suite of evaluated nuclear data sets. Van der Marck [39] recently provided an assessment of how ENDF/B-VII.1, JENDL-4.0, and JEFF-3.1 perform in MCNP6 simulations of over 2000 criticality ($k_{\rm eff}$) ICSBEP experiments, and of hundreds of neutron transmission and shielding experiments. Overall these libraries performed rather well, and we recognize that making improvements over the current libraries will be quite an accomplishment, especially since we will aim to avoid making any ad hoc evaluation decisions motivated solely by a desire to match an integral experiment. Rather, our goal is to obtain improved integral performance whilst at the same time also using improved microscopic nuclear physics in our ENDF-formatted CIELO files.

In addition to studying a wide range of $k_{\rm eff}$ integral criticality experiments that use different neutron spectra (fast, intermediate, thermal) and different materials (HEU, LEU, Pu, solutions, *etc.*), we will also include beta-eff, Rossi-alpha, reaction rate measurements (fission ratios, $(n, 2n)$ dosimetry responses, *etc.*), and shielding and neutron transmisison experiments. Data from PROFIL and MANTRA post-irradiation experiments can provide valuable guidance for capture and $(n, 2n)$ reactions. Other "semi-integral" experiments that isolate certain nuclear reaction quantities will also be studied, such as RPI's experiments that are sensitive to neutron scattering angular distributions, and subcritical neutron multiplication experiments that may be especially sensitive to $\overline{\nu}$.

Some of the recent data adjustment investigations will also play an important role in guiding CIELO work [81, 82]. These efforts have used recently created evaluated libraries of cross sections and covariances, and have investigated feedback from a wide range of critical assemblies that explore different materials and neutron energy spectra. The goal of such projects is to identify possible physically-important guidance that comes from these integral data (criticality, reaction rates, and so on), so as to improved the underlying nuclear cross sections and remove compensating errors. The work of the NEA/WPEC Subgroup 39 in this area will therefore be closely coordinated with our CIELO collaboration goals.

VI. ANALYSIS OF INTEGRAL QUANTITIES

Precise knowledge of neutron physics quantities plays an important role in the assessment of neutron evaluations for CIELO. Their numerical values can be extracted from the international collection of evaluated reaction libraries (ENDF/B-VII.1 [1], JEFF-3.1 [2], JENDL-4.0 [4], ROSFOND [5], CENDL-3.1 [6], and EAF-2010 activation file [94]) and compared.

In the present work, we consider neutron fission (n, f) and capture (n, γ) reactions and several parameters that are important for nuclear science and technology applications. Numerical values of thermal neutron cross sections (σ^{2200}), Westcott factors (g_w), resonance integrals (RI), Maxwellian-averaged cross sections, and ^{252}Cf spontaneous fission (sf) neutron spectrum averaged cross sections were produced in a systematic approach for nuclei of interest using the evaluated nuclear reaction data, Doppler broadened at 293.6 K. The complete description of this work for Z = 1–100 is given in Refs. [95, 96]. In this section, we will concentrate on the analysis of ^{1}H, ^{16}O, ^{56}Fe, ^{235}U, ^{238}U, and ^{239}Pu.

A. Thermal cross sections

Neutron thermal cross section values for fission and capture are shown in Fig. 8, and Tables II - III. These values are compared with *Atlas of Neutron Resonances* and *Neutron Cross Section Standards* evaluations [11, 28].

Further analysis of fission cross sections shows a disagreement between *Atlas of Neutron Resonances* [28] and ENDF/B-VII.1 thermal fission cross sections for ^{238}U. In this case the fission threshold is well above the thermal energy, but sub-threshold thermal neutron fission takes place. The experimental measurement of D'Hondt *et al.* [98] (11±2 micro-barns) is a lower value than that given in the ENDF/B-VII.1 library, indicating that more work is needed here.

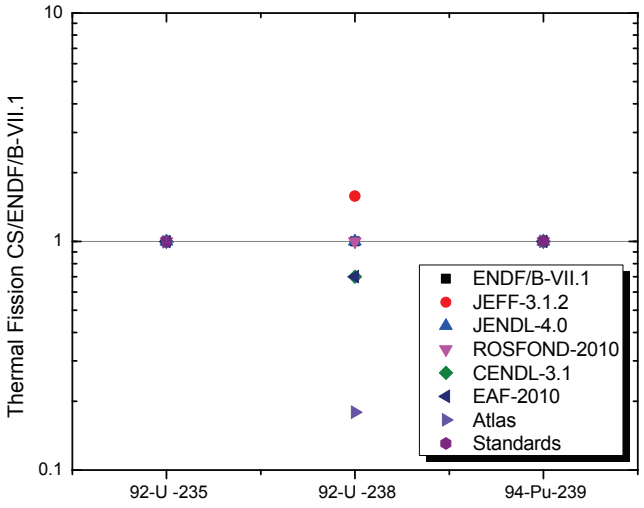

FIG. 8. Ratio of thermal neutron fission cross sections to ENDF/B-VII.1.

Thermal capture cross sections are consistent with ENDF/B-VII.1 values with the exception of ^{16}O, ^{238}U evaluations in EAF-2010.

B. Westcott Factors

The Westcott g-factor, g_w, is the ratio of the Maxwellian-averaged cross section to the 2200 m/s (thermal) cross section. The g_w-factor is temperature dependent and its value is close to 1 for most nuclei where $\sigma \sim 1/v$. Calculated Westcott factors are shown in Fig. 9, and Tables II - III.

Complete calculation of capture and fission g_w factors reveals that most of them are close to 1 with the exception of non-$1/v$ $\sigma(n,\gamma)$ nuclei: ^{113}Cd, ^{135}Xe, ^{149}Sm, ^{151}Eu, ^{176}Lu, ^{182}Ta, ^{239}Pu, ^{249}Bk [28]. Strong resonances in the thermal energy region, such as the 0.29562 eV resonance in ^{239}Pu [28], are often responsible for Westcott factor temperature variations.

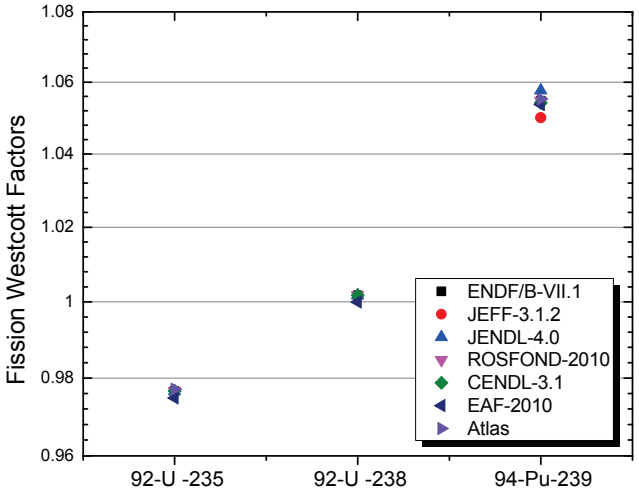

FIG. 9. Thermal neutron fission Westcott factors.

Deviations from unity for thermal fission Westcott factors are shown in Fig. 9. For ^{235}U, the fission Westcott factor is in agreement with the *Atlas* value of 0.9771±0.0008 [28].

C. Resonance Integrals

The epicadmium dilute resonance integral [28, 97] for a particular reaction $\sigma_R(E)$ in a $1/E$ spectrum is expressed by

$$\mathrm{RI} = \int_{E_c}^{\infty} \sigma_R(E) \frac{dE}{E}, \qquad (1)$$

where E_c is determined by cadmium cut-off energy (E_c=0.5 eV). Fig. 10, and Tables II - III show resonance integrals for fission, and capture. To satisfy the requirements of evaluation and research communities resonance integrals are calculated with the aid of Eq. (1) with an upper energy limits of 100 keV and 20 MeV, respectively. For capture reactions, the dominant contribution to this integral comes from the energy region below a few keV. In contrast, for threshold reactions and sub-threshold fission this is not the case, since the major contribution comes from the energy region above the threshold energy.

Most of the integrals reproduce the available data with a few exceptions. Table III shows evaluated library capture integral values for ^{16}O, and they are in fair agreement. At the same time the ENDF/B-VII.1 ^{16}O RI value of 7.380×10^{-4} b strongly disagrees with the calculated *Atlas* value of $2.700\times10^{-4}\pm3.000\text{x}10^{-5}$ b. The latter value does not include direct capture effects which were incorporated into the ENDF/B-VII.1 evaluation following JENDL-4.0.

TABLE II. Comparison of Evaluated Libraries Neutron **Fission** Integral Quantities and Experimental Benchmarks (C-calculated value). The uncertainties on the evaluated quantities were systematically calculated for ENDF/B-VII.1 as an illustration of the current knowledge of evaluated data.

Quantity	Library	ENDF Materials		
		^{235}U	^{238}U	^{239}Pu
σ^{2200} (b)	ENDF/B-VII.1	(5.850±0.020)E+2	(1.680±1.048)E-5	(7.479±0.081)E+2
	JEFF-3.1.1	5.850E+2	2.651E-5	7.471E+2
	JENDL-4.0	5.851E+2	1.680E-5	7.474E+2
	ROSFOND	5.851E+2	1.680E-5	7.479E+2
	CENDL-3.1	5.850E+2	1.178E-5	7.471E+2
	EAF-2010	5.832E+2	1.178E-5	7.477E+2
	Atlas [28]	(5.826±0.011)E+2	3.000E-6^C	(7.481±0.020)E+2
	Standards [11]	(5.843±0.010)E+2		(7.500±0.018)E+2
g_w	ENDF/B-VII.1	9.767E-1	1.002E+0	1.055E+0
	JEFF-3.1.1	9.767E-1	1.001E+0	1.050E+0
	JENDL-4.0	9.765E-1	1.002E+0	1.058E+0
	ROSFOND	9.765E-1	1.002E+0	1.055E+0
	CENDL-3.1	9.767E-1	1.002E+0	1.054E+0
	EAF-2010	9.748E-1	1.000E+0	1.054E+0
	Atlas [28]	(9.771±0.008)E-1		(1.055±0.001)E+0
$\int_{0.5eV}^{100keV}$ RI (b)	ENDF/B-VII.1	(2.687±0.008)E+2	(2.340±0.428)E-3	(2.931±0.021)E+2
	JEFF-3.1.1	2.688E+2	1.217E-3	2.932E+2
	JENDL-4.0	2.686E+2	2.349E-3	2.930E+2
	ROSFOND	2.689E+2	2.340E-3	2.928E+2
	CENDL-3.1	2.688E+2	1.895E-3	2.893E+2
	EAF-2010	2.716E+2	2.159E-3	2.926E+2
$\int_{0.5eV}^{20MeV}$ RI (b)	ENDF/B-VII.1	(2.760±0.008)E+2	(2.054±0.012)E+0	(3.027±0.022)E+2
	JEFF-3.1.1	2.760E+2	2.059E+0	3.028E+2
	JENDL-4.0	2.757E+2	2.029E+0	3.026E+2
	ROSFOND	2.762E+2	2.054E+0	3.025E+2
	CENDL-3.1	2.760E+2	2.022E+0	2.990E+2
	EAF-2010	2.788E+2	2.024E+0	3.024E+2
	Atlas [28]	(2.750±0.050)E+2	(1.63±0.16)E-3^C	(3.030±0.100)E+2
MACS, $kT = 30keV$ (b)	ENDF/B-VII.1	(2.204±0.013)E+0	(7.988±0.336)E-5	(1.822±0.006)E+0
	JEFF-3.1.1	2.213E+0	7.173E-5	1.809E+0
	JENDL-4.0	2.169E+0	7.566E-5	1.836E+0
	ROSFOND	2.219E+0	7.989E-5	1.808E+0
	CENDL-3.1	2.216E+0	7.532E-5	1.843E+0
	EAF-2010	2.213E+0	1.206E-4	1.806E+0
$\overline{\sigma}$ ^{252}Cf(sf) (b)	ENDF/B-VII.1	(1.209±0.019)E+0	(3.117±0.040)E-1	(1.774±0.027)E+0
	JEFF-3.1.1	1.203E+0	3.102E-1	1.774E+0
	JENDL-4.0	1.202E+0	3.094E-1	1.777E+0
	ROSFOND	1.211E+0	3.115E-1	1.771E+0
	CENDL-3.1	1.202E+0	3.097E-1	1.786E+0
	EAF-2010	1.200E+0	3.078E-1	1.786E+0
	EXFOR [99]	(1.215±0.022)E+0	(3.109±0.140)E-1	(1.790±0.041)E+0

It is important to note that for ^{238}U target nucleus, where sub-threshold fission was observed, the calculated fission integrals I_f^c reported in the *Atlas of Neutron Resonances* [28] correspond to subthreshold fission values.

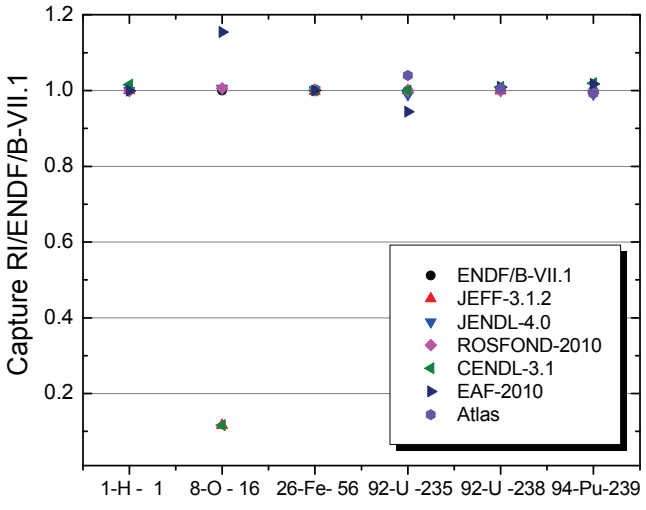

FIG. 10. Ratio of neutron capture resonance integrals to ENDF/B-VII.1.

D. Maxwellian-averaged cross sections

Maxwellian-averaged cross sections have been calculated for the temperature (kT) of 30 keV. This temperature is the commonly accepted value in stellar nucleosynthesis s-process compilations. Analysis of calculated MACS and experimental data provides an important tool for ENDF quality assurance.

The neutron capture MACS are shown in Fig. 11. There is no reliable source for fission MACS besides the evaluated nuclear library values. The stellar nucleosynthesis KADoNiS library [100] contains only neutron capture MACS for the ^{1}H and ^{210}Po range of nuclei. The analysis of fission cross sections in Table II indicates potential issues with the JEFF-3.1 library for ^{238}U, where sub-threshold fission cross section is underestimated.

A detailed analysis of Fig. 11 demonstrates the nuclear astrophysics potential of ENDF libraries as a complementary source of evaluated cross sections and reaction rates [96]. There are noticeable differences between KADoNiS [100] and ENDF/B-VII.1 libraries for light and medium nuclei. The ^{1}H deviation is due to differences between center of mass (ENDF calculated) and lab reference system (KADoNiS) cross section values, and therefore, this is not a discrepancy. Owing to a lack of resonances in the

TABLE III. Comparison of Evaluated Libraries Neutron **Capture** Integral Quantities and Experimental Benchmarks (R-relative measurement, C-calculated value). The uncertainties on the evaluated quantities were systematically calculated for ENDF/B-VII.1 as an illustration of the current knowledge of evaluated data.

Quantity	Library	ENDF Materials					
		^{1}H	^{16}O	^{56}Fe	^{235}U	^{238}U	^{239}Pu
σ^{2200} (b)	ENDF/B-VII.1	(3.320±0.085)E-1	(1.900±0.190)E-4	(2.589±0.140)E+0	(9.869±0.162)E+1	(2.863±0.053)E+0	(2.707±0.041)E+2
	JEFF-3.1.1	3.320E-1	1.900E-4	2.586E+0	9.869E+1	2.684E+0	2.728E+2
	JENDL-4.0	3.320E-1	1.899E-4	2.591E+0	9.871E+1	2.683E+0	2.715E+2
	ROSFOND	3.320E-1	1.899E-4	2.591E+0	9.871E+1	2.683E+0	2.707E+2
	CENDL-3.1	3.320E-1	1.900E-4	2.589E+0	9.869E+1	2.718E+0	2.704E+2
	EAF-2010	3.320E-1	2.020E-4	2.591E+0	9.895E+1	2.720E+0	2.705E+2
	Atlas [28]	(3.326±0.007)E-1	(1.900±0.200)E-4	(2.590±0.140)E+0	(9.880±0.080)E+1	(2.680±0.019)E+0	(2.693±0.029)E+2
	Standards [11]				(9.940±0.072)E+1	(2.677±0.013)E+0	(2.715±0.021)E+2
g_w	ENDF/B-VII.1	1.001E+0	1.001E+0	1.000E+0	9.913E-1	1.002E+0	1.146E+0
	JEFF-3.1.1	1.001E+0	1.001E+0	1.000E+0	9.913E-1	1.002E+0	1.146E+0
	JENDL-4.0	1.001E+0	1.001E+0	1.001E+0	9.911E-1	1.002E+0	1.142E+0
	ROSFOND	1.001E+0	1.001E+0	1.001E+0	9.911E-1	1.002E+0	1.146E+0
	CENDL-3.1	1.001E+0	1.001E+0	1.000E+0	9.913E-1	1.003E+0	1.146E+0
	EAF-2010	9.995E-1	9.996E-1	9.987E-1	9.833E-1	1.001E+0	1.144E+0
	Atlas [28]				(9.956±0.016)E-1	(1.0009E+0^{C})	1.130E+0
$\int_{0.5eV}^{100keV}$ RI (b)	ENDF/B-VII.1	(1.490±0.038)E-1	(1.525±0.153)E-4	(1.329±0.133)E+0	(1.398±0.015)E+2	(2.752±0.040)E+2	(1.811±0.016)E+2
	JEFF-3.1.1	1.490E-1	8.538E-5	1.327E+0	1.398E+2	2.750E+2	1.811E+2
	JENDL-4.0	1.490E-1	1.588E-4	1.330E+0	1.383E+2	2.752E+2	1.793E+2
	ROSFOND	1.490E-1	1.588E-4	1.330E+0	1.398E+2	2.752E+2	1.811E+2
	CENDL-3.1	1.512E-1	8.538E-5	1.329E+0	1.398E+2	2.777E+2	1.846E+2
	EAF-2010	1.489E-1	1.724E-4	1.328E+0	1.320E+2	2.777E+2	1.841E+2
$\int_{0.5eV}^{20MeV}$ RI (b)	ENDF/B-VII.1	(1.492±0.038)E-1	(7.380±1.658)E-4	(1.346±0.134)E+0	(1.404±0.016)E+2	(2.756±0.040)E+2	(1.814±0.016)E+2
	JEFF-3.1.1	1.492E-1	8.556E-5	1.343E+0	1.405E+2	2.753E+2	1.815E+2
	JENDL-4.0	1.492E-1	7.427E-4	1.349E+0	1.390E+2	2.756E+2	1.797E+2
	ROSFOND	1.492E-1	7.427E-4	1.350E+0	1.404E+2	2.756E+2	1.815E+2
	CENDL-3.1	1.515E-1	8.556E-5	1.347E+0	1.404E+2	2.780E+2	1.849E+2
	EAF-2010	1.491E-1	8.522E-4	1.346E+0	1.326E+2	2.781E+2	1.846E+2
	Atlas [28]		(2.700±0.300)E-4^{C}		(1.460±0.060)E+2	(2.770±0.030)E+2	(1.800±0.200)E+2
MACS, $kT = 30keV$ (b)	ENDF/B-VII.1	(1.525±0.059)E-4	(3.154±0.325)E-5	(1.151±0.118)E-2	(6.926±2.244)E-1	(4.004±0.062)E-1	(5.278±0.549)E-1
	JEFF-3.1.1	1.524E-4	1.695E-7	1.148E-2	6.947E-1	3.970E-1	5.519E-1
	JENDL-4.0	1.525E-4	3.155E-5	1.184E-2	7.048E-1	3.989E-1	5.400E-1
	ROSFOND	1.525E-4	3.15E-5	1.217E-2	6.926E-1	4.004E-1	5.517E-1
	CENDL-3.1	1.525E-4	1.695E-7	1.151E-2	6.953E-1	3.992E-1	5.165E-1
	EAF-2010	1.523E-4	3.585E-5	1.151E-2	6.930E-1	4.011E-1	5.651E-1
	KADONIS [100]	(2.540±0.200)E-4	(3.800±0.400)E-5	(1.170±0.050)E-2			
$\overline{\sigma}$ ^{252}Cf(sf) (b)	ENDF/B-VII.1	(3.872±1.452)E-5	(1.119±1.073)E-4	(2.893±0.255)E-3	(9.025±1.870)E-2	(6.720±0.142)E-2	(3.870±0.679)E-2
	JEFF-3.1.1	3.865E-5	2.827E-8	2.634E-3	9.031E-2	6.632E-2	5.194E-2
	JENDL-4.0	3.871E-5	1.117E-4	3.316E-3	8.470E-2	6.802E-2	5.105E-2
	ROSFOND	3.871E-5	1.117E-4	3.174E-3	9.012E-2	6.716E-2	5.181E-2
	CENDL-3.1	3.764E-5	2.827E-8	3.125E-3	7.611E-2	6.765E-2	5.118E-2
	EAF-2010	3.864E-5	7.929E-5	2.893E-3	9.017E-2	6.675E-2	6.880E-2
	EXFOR [99]	(7.418±0.526)E-5^{R}					

radiative capture cross sections of JEFF-3.1 and CENDL-3.1 ^{16}O evaluations, the corresponding neutron capture MACS strongly deviate from the rest.

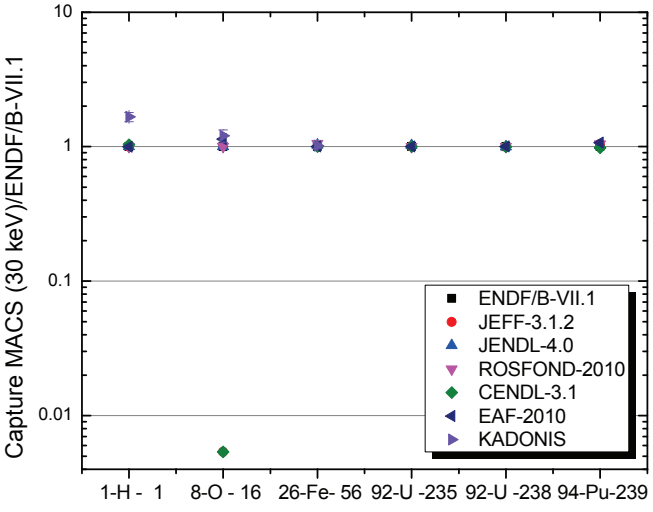

FIG. 11. Ratio of calculated MACS at kT =30 keV and KADoNiS data to ENDF/B-VII.1 for neutron-induced capture reactions.

E. ^{252}Cf(sf) cross sections

The californium neutron source provides a pure fission neutron spectrum. This is very useful for validation tests of evaluated data in the fast region, even though it is not representative of a fast reactor spectrum (being hotter). Selected fission neutron spectrum-averaged experimental data have been compiled in the EXFOR database [99].

Many experimental spectrum-averaged cross sections have been evaluated by the dosimetry community [12, 46, 101]. In this work, we used Mannhart's evaluation [101] of the ^{252}Cf(sf) neutron spectrum. As is shown in Tables II - III, the calculated californium spectrum-averaged cross sections exhibit reasonable agreement with measurements. However, spectrum-averaged cross section measurements of this type below 2 MeV are very difficult due to increased neutron scattering and background; measurements above 8 MeV become difficult due to reduced neutron flux. Therefore both capture and fission measurements in a Cf spectrum should be taken with care. New spectrum-averaged cross section measurements in a Cf-spectrum are encouraged, to improve our database and to provide a better validation of our cross section evaluations. We also note that small differences in various computational methods for calculating the cal-

ifornium spectrum-averaged cross sections, together with variations in measured values, leads to some small differences in Table II (from Pritychenko) relative to Capote *et al.*'s values [102] that also uses ENDF/B-VII.0 (which is the same as VII.1 for fission). For example, for fission, Capote *et al.* have: ^{235}U(n,f) calc. 1.225±0.4% b, exp. 1.210±1.2% b; ^{238}U(n,f) calc. 0.3185±0.6% b, exp. 0.3257±1.6% b; ^{239}Pu(n,f) calc. 1.796±0.5% b, exp. 1.812±1.4% b.

We also note that for capture, the ^{239}Pu(n,γ) reaction needs work and ENDF/B-VII.1 appears to be discrepant compared to the other evaluations; however, there are few measured data to compare against.

VII. CONCLUSIONS

We are proposing a closer international cooperation for evaluating nuclear data. This will ultimately benefit nuclear data users through the creation of a higher fidelity database. Our long-term objective is to create the international nuclear data library CIELO (Collaborative International Evaluated Library Organization), and as the first step we focused in this paper on indentifying discrepancies in the evaluations for ^{1}H, ^{16}O, ^{56}Fe, ^{235,238}U, and ^{239}Pu among the evaluated nuclear data libraries (ENDF/B-VII.1, JEFF-3.1, JENDL-4.0, CENDL-3.1, and ROSFOND). We anticipate that this collaboration will help identify future experiments that are needed — from cross section measurements (*e.g.*, as collated in the NEA's High Priority Request List) to more integral experiments. The next step is to put together teams of specialists to resolve these discrepancies. This is now being done in the framework of the NEA WPEC in close collaboration with the IAEA-NDS for standards evaluations.

We thank P. Oblozinsky and A. Nichols for useful comments. This work was carried out under the auspices of the National Nuclear Security Administration of the US Department of Energy at Los Alamos National Laboratory under Contract No. DE-AC52-06NA25396, at Brookhaven National Laboratory under Contract No. DE-AC02-98CH10886, at Oak Ridge National Laboratory under Contract No. DE-AC05-00OR22725, and at Lawrence Livermore National Laboratory under Contract DE-AC52-07NA27344. R. Vogt also acknowledges the Physics Department, University of California at Davis for support.

[1] M. B. Chadwick *et al.*, Nucl. Data Sheets **112**, 2887 (2011).
[2] A.J. Koning *et al.*, JEFF Report **21**, NEA (2006).
[3] A.J. Koning *et al.*, JEFF Report **23**, NEA (2013).
[4] K. Shibata *et al.*, J. Nucl. Sci. Technol. **48**, 1 (2011).
[5] S.V. Zabrodskaya, *et al.*, Nucl. Const. **1-2**, 3 (2007).
[6] Z.G. Ge *et al.*, J. Korean Phys. Soc. **59**, No. 2, 1052 (2011).
[7] A. Plompen *et al.*, IAEA report INDC(NDS)-0597 (2012).
[8] E. Bauge *et al.*, Eur. Phys. J. A **48**, 113 (2012).
[9] R.D. Mosteller, Los Alamos National Laboratory Report LA-UR-10-06230 (2010).
[10] T. Goorley *et al.*, Nucl. Tech. **180**, 298 (2012).
[11] A. D. Carlson *et al.*, Nucl. Data Sheets **110**, 3215 (2009).
[12] R. Capote *et al.*, J. ASTM International (JAI), JAI104119 (2012).
[13] R.A. Forrest *et al.*, IAEA report INDC(NDS)-0628 (2012).
[14] P. Oblozinsky *et al.*, NEA/WPEC-23 (2009).
[15] Y. Kanda *et al.*, NEA/WPEC-4 (1999).
[16] R. Capote *et al.*, Nucl. Data Sheets **110**, 3107 (2009).
[17] Compilation of plots of the main nuclear data prepared by NNDC, available from http://www.oecd-nea.org/science/wpec/sg40-cielo (2012).
[18] N. Boukharouba *et al.*, Phys. Rev. C **65**, 014004 (2002).
[19] N. Boukharouba *et al.*, Phys. Rev. C **82**, 014001 (2010).
[20] R. A. Arndt *et al.*, Phys. Rev. D **45**, 3995 (1992).
[21] V. G. J. Stoks *et al.*, Phys. Rev. C **48**, 792 (1993).
[22] G. Giorginis *et al.*, EDP Science, 525 (2008).
[23] J. K. Bair and F. X. Haas, Phys. Rev. C **7**, 1356 (1973).
[24] A. Kahler *et al.*, Nucl. Data Sheets **112**, 2997 (2011).
[25] S. Harissopulos *et al.*, Phys. Rev. C **72**, 062801(R) (2005).
[26] M. Igshira *et al.*, Astrophys. J. Part 2, Letters, **441** No 2., L89-L92 (1995).
[27] W. Dilg, *et al.*, Phys. Lett. B **36** 208 (1971).
[28] S.F. Mughabghab, Atlas of Neutron Resonances, Elsevier (2006).
[29] A. Plompen, WINS2010 conference, Strasbourg, France (2010); JEF/DOC-1488 (2013).
[30] C. Lubitz, CSEWG (November 2012).
[31] C. Lubitz, CSEWG (2008).
[32] K. Kozier, D. Roubtsov, A Plompen, S. Kopecky, Proc. PHYSOR 2012 - Advances in Reactor Physics, April 15-20 (2012).
[33] M.T. Wenner *et al.*, Nucl. Sci. Eng. **170** 207 (2012).
[34] F.S. Dietrich *et al.*, Phys. Rev. C **68**, 064608 (2003).
[35] E.S. Soukhovitskii *et al.* J. Nucl. Sci. Technol. **39** (2002).
[36] S. Kunieda *et al.*, Phys. Rev. C **85**, 054602 (2012).
[37] M. B. Chadwick *et al.*, Nucl. Data Sheets **107**, 2931 (2006).
[38] G. Chiba *et al.*, J. Nucl. Sci. Technol. **48**, 172 (2011).
[39] S.C. van der Marck, Nucl. Data Sheets **113**, 2935 (2012).
[40] J. Rowlands and C. Nordborg, NEACRP-A-1011, NEANDC-A-257, Nuclear Energy Agency, OECD (1989).
[41] V. Maslov *et al.*. J. Korean Phys. Soc. **59** No. 2, 1337 (2011).

[42] T. Ohsawa, Nucl. Phys. A **665**, 3 (2000).
[43] G. Vladuca and A.Tudora, Ann. Nucl. Energy **28**, 689 (2001).
[44] R. Capote, IAEA INDC(NDS)-0571 (2010).
[45] M.B. Chadwick *et al.*, Nucl. Data Sheets **108**, 2716 (2007).
[46] K.I. Zolotarev, IAEA report, INDC(NDS)-0526 (2008); IAEA report, INDC(NDS)-0546 (2009); IAEA report, INDC(NDS)-0584 (2010).
[47] J.P. Lestone and E. Shores, Nucl. Data Sheets **115**, xxx this issue (2014).
[48] T. Kawano *et al.*, Phys. Rev. C **63**, 034601 (2001).
[49] O. Iwamoto, J. Nucl. Sci. Technol. **45** 910 (2008).
[50] J.L. Ullmann *et al.*, Phys. Rev. C **87**, 044607 (2013).
[51] S. Lemaire *et al.*, Phys. Rev. C **72**, 024601 (2005).
[52] S. Lemaire *et al.*, Phys. Rev. C **73**, 014602 (2006).
[53] R. Vogt *et al.*, Phys. Rev. C **87**, 054903 (2013).
[54] R. Vogt *et al.*, Phys. Rev. C **85**, 024608 (2012).
[55] K.H. Schmidt *et al.*, Phys. Rev. C **83**, 061601(R) (2011).
[56] M. Baba *et al.*, J. Nucl. Sci. Technol. **27**, 601 (1990).
[57] M. Baba *et al.*, Proc. Int. Conf. Nuclear Data for Science and Technology, Jülich, Germany, 13–17 May 1991, p.349 (1991).
[58] P. G. Young *et al.*, Nucl. Data Sheets **108**, 2589 (2007).
[59] J.L. Kammerdiener, Lawrence Livermore National Laboratory report UCRL-51232 (1972).
[60] T. Kawano *et al.*, Proc. of the 1993 Symposium on Nuclear Data, 18–19 Nov., 1993, JAERI, Tokai, Japan, Ed. M. Kawai and T. Fukahori, JAERI-M 94-019, pp.290–299 (1994).
[61] K. Shibata *et al.*, J. Nucl. Sci. Technol. **39**, 1125 (2002).
[62] M. Dupuis *et al.*, Proc. Int. Conf. Nuclear Reaction Mechanisms, June 11 – 15, 2012, Varenna, Italy (2012).
[63] H. Wienke *et al.*, Phys. Rev. C **78**, 064611 (2008).
[64] S.P. Simakov *et al.*, Proc. Int. Conf. Nuclear Data for Science and Technology, Apr. 22–27, 2007, Nice, France, Eds. O. Bersillon, F. Gunsing, E. Bauge, R. Jacqmin, and S. Leray, EDP Science, p.845 (2008).
[65] L.C. Leal *et al.*, Oak Ridge National Laboratory report ORNL/TM-13516 (1997); Nucl. Sci. Eng. **131**, 230 (1999).
[66] L.C. Leal *et al.*, Nucl. Sci. Eng. **109**, 1 (1991).
[67] O. Iwamoto *et al.*, Nucl. Data Sheets **115**, xxx (2014).
[68] M. Jandel *et al.*, Phys. Rev. Lett. **109**, 202506 (2012).
[69] J. Tommasi, E. Dupont, P. Marimbeau, Nucl. Sci. Eng. **154**, 119 (2006).
[70] P.G. Young *et al.*, Los Alamos National Laboratory report LA-12343-MS (1992).
[71] Go Chiba, MCNP/ENDF/NJOY Workshop, Los Alamos, October 30 - Nov 1, 2012.
[72] J. Frehaut, NEANDC(E) 238/L (1986).
[73] H. Vonach *et al.* NUCL. SCI. ENG. 106, 409 (1990).
[74] W. Younes *et al.*, Lawrence Livermore National Laboratory report UCRL-140313 (2000).
[75] R. Gwin *et al.*, Oak Ridge National Laboratory report ORNL-TM-6246 (1978).
[76] R. Gwin *et al.*, Nucl. Sci. Eng. **87**, 381 (1984).
[77] E. Bauge, private communication. P. Casoli, Nucl. Data Sheets **115**, xxx (2014).
[78] H. Derrien *et al.*, Proc. Int. Conf. on Nuc. Data for Sci. and Tech., Santa-Fe, USA (2004).
[79] Y. Nagaya, MCNP/ENDF/NJOY Workshop, Los Alamos, October 30 - Nov 1, 2012.
[80] K. Sugino, M. Ishikawa *et al.*, JAEA-Research report 2012-013 (2012).
[81] M. Salvatores, *et al.*, Nucl. Data Sheets **115**, xxx (2014).
[82] G. Palmiotti, *et al.*, Nucl. Data Sheets **115**, xxx (2014).
[83] J.D. Knight *et al.*, Phys. Rev. **112**, 259 (1958).
[84] N.V. Kornilov *et al.*, Zentralinstut für Kernforschung Rossendorf Report No.410, p.68 (1980).
[85] C. Zhu *et al.*, Nucl. Sci. Eng. **169**, 188 (2011).
[86] H.D. Selby *et al.* Nucl. Data Sheets **111**, 2891 (2010).
[87] H. Derrien, L.C. Leal, and N.M. Larson, Proc. Int. Conf. Nuclear Data for Science and Technology, Apr. 22–27, 2007, Nice, France, Eds. O. Bersillon, F. Gunsing, E. Bauge, R. Jacqmin, and S. Leray, EDP Science, p.667 (2008).
[88] J.C. Hopkins, B.C. Diven, Nucl. Sci. Eng. **12**, 169 (1962).
[89] R. Batchelor and K. Wyld, A.W.R.E. Aldermaston Reports, AWRE-O-55/69, (1969).
[90] V.N. Andreev, Prog. Neutron Phys., New York, p. 211 (1961) USA.
[91] J.A. Becker *et al.*, J. Nucl. Sci. Technol. Suppl. **2**, 620 (2002).
[92] R. Lougheed *et al.*, Radiochim. Acta **90**, 833 (2002).
[93] D. Rochman and A. J. Koning, Nucl. Sci. Eng. **169**, 68 (2011).
[94] J.-Ch. Sublet *et al.*, EASY Documentation Series CCFE-R (10) 05, April 2010.
[95] B. Pritychenko and S.F. Mughabghab, Nucl. Data Sheets **113**, 3120 (2012).
[96] B. Pritychenko *et al.*, At. Data Nucl. Data Tables **96**, 645 (2010).
[97] D.J. Hughes, Pile Neutron Research, Addison Wesley (1953).
[98] P. D'Hondt *et al.*, Ann. Nucl. Energy **11**, 485 (1984).
[99] International Network of Nuclear Reaction Data Centres (NRDC), "Compilation of Experimental Nuclear Reaction Data (EXFOR/CSISRS)", (Available from http://www-nds.iaea.org/exfor/, http://www.nndc.bnl.gov/exfor/). N. Otuka *et al.*, Nucl. Data Sheets **115**, xxx (2014).
[100] I. Dillmann *et al.*, AIP Conf. Proc. **819**, 123 (2006); Data downloaded from http://www.kadonis.org on April 14, 2011.
[101] W. Mannhart, International Atomic Energy Agency Report IAEA-TECDOC-410, IAEA, Vienna, 158 (1987). Nucl. Data for Sci. and Tech., 429 (1983).
[102] R. Capote *et al.*, Proc. Int. Symposium on Reactor Dosimetry, Bretton Woods, NH, USA, 22-27 May (2011); J. of ASTM International **9** JAI104119 (2012).
[103] S. Frankle *et al.*, Los Alamos National Laboratory report LA-13675 (1999).
[104] M. MacInnes *et al.*, Los Alamos National Laboratory report (in preparation).

Appendix A: Updated Results of LANL Integral Experiments

In this appendix we provide measured experimental data obtained at Los Alamos National Laboratory on activation and fission cross sections within fast critical assemblies. These data were used in Figs. 5 and 7.

TABLE IV. 14.1 MeV cross sections (barns) used in the calibration process for determining activation cross sections in critical assemblies. The pre-1963 and post-1963 values were those in use at the time by Los Alamos radiochemists. The uncertainties adopted were taken from various sources: ENDF/B-VII.1, IRDFF, or internal LANL estimates.

Reaction	Los Alamos		ENDF/B	
	pre-1963	post-1963	VII.1	Unc.(%)
^{45}Sc$(n,2n)^{44m}$Sc	0.115	0.105	0.104	5.0
^{51}V$(n,\alpha)^{48}$Sc	0.0157		0.0152	5.0
^{75}As$(n,2n)^{74}$As	1.050		0.994	5.0
^{89}Y$(n,2n)^{88}$Y	0.670	0.845	0.850	2.1
^{90}Zr$(n,2n)^{89}$Zr	0.643	0.590	0.617	0.91
^{103}Rh$(n,2n)^{102g}$Rh	0.750	0.783	0.741	5.0
^{107}Ag$(n,2n)^{106m}$Ag		0.573	0.520	5.0
^{169}Tm$(n,2n)^{168}$Tm		1.96	1.980	1.7
^{175}Lu$(n,2n)^{174}$Lu		1.789	2.122	5.0
^{191}Ir$(n,2n)^{190}$Ir[a]		1.995	2.066	3.0
^{197}Au$(n,2n)^{196}$Au		2.214	2.132	1.1
^{203}Tl$(n,2n)^{202}$Tl	1.428	2.090	2.005	5.0
^{204}Pb$(n,2n)^{203}$Pb	1.746		2.193	5.0
^{238}U$(n,2n)^{237}$U		0.895	0.850	2.4

[a] 190g+m1+m2+8.6%m3 is measured, see Ref. [45], Fig. 13.

TABLE V. Reaction rate measurements in plutonium Jezebel critical assemblies.

Assembly/date	Reaction	Measurement
Jezebel	^{239}Pu$(n,f)/^{235}$U(n,f)	1.430
10/23/1973	^{169}Tm$(n,2n)/^{235}$U(n,f)	3.125E-03
	^{191}Ir$(n,2n)/^{235}$U(n,f)	3.206E-03
	^{238}U$(n,2n)/^{235}$U(n,f)	1.058E-02[a]
	^{238}U$(n,f)/^{235}$U(n,f)	2.121E-01

[a] Values we gave in NDS 108, 2587 (2007) Table IX (∼1.42E-02) for ^{238}U$(n,2n)$ were erroneous. We apologize – those values were for Jezebel-33.

By comparing MCNP model calculations of these reactions (using ENDF/B-VII.1) with our measurements, we can assess the accuracy of the ENDF/B-VII.1 $(n,2n)$ cross sections, the prompt fission neutron spectra (PFNS), and the neutronic transport modeling. The value of these data in particular relates to insights that are provided on the accuracy of our PFNS. This is because we focus on the use of activation dosimetry reactions where the $(n,2n)$ cross sections are well known. Also, we aim to use a number of different dosimetry reactions so that even if one evaluated cross section is biased in some way, we benefit from using feedback from the ensemble of reactions.

The measurements reported here are old and were carried out in the 1960s and 1970s. Some of them have

TABLE VI. Reaction rate measurements in plutonium Flattop-Pu critical assemblies.

Assembly/date	Reaction	Measurement
Flattop-Pu	^{239}Pu$(n,f)/^{235}$U(n,f)	1.415
8/10/1967	^{169}Tm$(n,2n)/^{235}$U(n,f)	2.433E-03
	^{203}Tl$(n,2n)/^{235}$U(n,f)	2.270E-03
	^{107}Ag$(n,2n)^{106m}$Ag$/^{235}$U(n,f)	1.973E-04
8/5/1970	^{238}U$(n,f)/^{235}$U(n,f)	(1.484E-01)[a]
	^{191}Ir$(n,2n)/^{235}$U(n,f)	2.831E-03
8/5/1963	^{238}U$(n,2n)/^{235}$U(n,f)	9.041E-03
3/25/1962	^{238}U$(n,f)/^{235}$U(n,f)	1.712E-01
	^{238}U$(n,2n)/^{235}$U(n,f)	8.989E-03

[a] We do not recommend using this value as it appears to be erroneous and is discrepant with the 0.1712 value shown. This spectral index value should be larger than the values in Flattop-25 but it is not.

TABLE VII. Reaction rate measurements in the HEU Godiva critical assembly.

Assembly/date	Reaction	Measurement
Godiva	^{238}U$(n,2n)/^{235}$U(n,f)	7.729E-03
6/30/1959	^{238}U$(n,f)/^{235}$U(n,f)	1.629E-01
	^{239}Pu$(n,f)/^{235}$U(n,f)	1.365

TABLE VIII. Reaction rate measurements in the HEU Flattop-25 critical assemblies.

Assembly/date	Reaction	Measurement
Flattop-25	^{75}As$(n,2n)/^{235}$U(n,f)	1.543E-04
3/5/1962	^{103}Rh$(n,2n)^{102g}$Rh$/^{235}$U(n,f)	2.618E-04
	^{204}Pb$(n,2n)/^{235}$U(n,f)	1.635E-05
	^{51}V$(n,\alpha)/^{235}$U(n,f)	1.142E-05
	^{45}Sc$(n,2n)^{44m}$Sc$/^{235}$U(n,f)	9.017E-06
3/30/1962	^{75}As$(n,2n)/^{235}$U(n,f)	1.452E-04
	^{51}V$(n,\alpha)/^{235}$U(n,f)	1.087E-05
	^{45}Sc$(n,2n)^{44m}$Sc$/^{235}$U(n,f)	8.889E-06
4/29/1968	^{239}Pu$(n,f)/^{235}$U(n,f)	1.382
	^{169}Tm$(n,2n)/^{235}$U(n,f)	1.468E-03
	^{203}Tl$(n,2n)/^{235}$U(n,f)	1.535E-03
	^{107}Ag$(n,2n)^{106m}$Ag$/^{235}$U(n,f)	1.336E-04
4/7/1969	^{197}Au$(n,2n)/^{235}$U(n,f)	1.614E-03
	^{191}Ir$(n,2n)/^{235}$U(n,f)	1.828E-03

TABLE IX. Reaction rate measurements in the HEU Flattop-25 critical assembly traverse, 2/20/1961 (distance measured from center in cm).

Distance	Reaction	Measurement
0.4	^{238}U$(n,2n)/^{235}$U(n,f)	6.975E-03
1.03	^{238}U$(n,2n)/^{235}$U(n,f)	7.199E-03
3.69	^{238}U$(n,2n)/^{235}$U(n,f)	6.364E-03
5.6	^{238}U$(n,2n)/^{235}$U(n,f)	5.679E-03
6.32	^{238}U$(n,2n)/^{235}$U(n,f)	4.562E-03
7.7	^{238}U$(n,2n)/^{235}$U(n,f)	3.059E-03
12.78	^{238}U$(n,2n)/^{235}$U(n,f)	1.243E-03
0.4	^{238}U$(n,f)/^{235}$U(n,f)	0.1543
1.03	^{238}U$(n,f)/^{235}$U(n,f)	0.1560
3.69	^{238}U$(n,f)/^{235}$U(n,f)	0.1435
5.6	^{238}U$(n,f)/^{235}$U(n,f)	0.1266
6.32	^{238}U$(n,f)/^{235}$U(n,f)	0.1005
7.7	^{238}U$(n,f)/^{235}$U(n,f)	0.0710
12.78	^{238}U$(n,f)/^{235}$U(n,f)	0.0279

TABLE X. Reaction rate measurements in the HEU Flattop-25 critical assembly traverse, 3/13/1961 (distance measured from center in cm).

Distance	Reaction	Measurement
0.01	^{238}U$(n,2n)/^{235}$U(n,f)	6.826E-03
1.02	^{238}U$(n,2n)/^{235}$U(n,f)	6.765E-03
3.7	^{238}U$(n,2n)/^{235}$U(n,f)	6.459E-03
5.16	^{238}U$(n,2n)/^{235}$U(n,f)	5.963E-03
6.31	^{238}U$(n,2n)/^{235}$U(n,f)	4.531E-03
9.62	^{238}U$(n,2n)/^{235}$U(n,f)	1.641E-03
14.75	^{238}U$(n,2n)/^{235}$U(n,f)	8.676E-04
0.01	^{238}U$(n,f)/^{235}$U(n,f)	0.1502
1.02	^{238}U$(n,f)/^{235}$U(n,f)	0.1512
3.7	^{238}U$(n,f)/^{235}$U(n,f)	0.1421
5.16	^{238}U$(n,f)/^{235}$U(n,f)	0.1289
6.31	^{238}U$(n,f)/^{235}$U(n,f)	0.1002
9.62	^{238}U$(n,f)/^{235}$U(n,f)	0.0428
14.75	^{238}U$(n,f)/^{235}$U(n,f)	0.0206

TABLE XI. Reaction rate measurements of ^{203}Tl$(n,2n)$ in the HEU Flattop-25 critical assembly traverse, 2/20/1961 (distance measured from center in cm).

Distance	Reaction	Measurement
0.4	^{203}Tl$(n,2n)/^{235}$U(n,f)	1.558E-03
1.03	^{203}Tl$(n,2n)/^{235}$U(n,f)	1.571E-03
3.69	^{203}Tl$(n,2n)/^{235}$U(n,f)	1.466E-03
5.6	^{203}Tl$(n,2n)/^{235}$U(n,f)	1.251E-03
6.32	^{203}Tl$(n,2n)/^{235}$U(n,f)	1.059E-03
7.7	^{203}Tl$(n,2n)/^{235}$U(n,f)	6.884E-04
12.78	^{203}Tl$(n,2n)/^{235}$U(n,f)	3.471E-04

been reported before in our *Nuclear Data Sheets* papers [45, 58] and by Frankle [103], but in the course of this work we have found some additional measurements that we report here. Most importantly, we update the "historical" LANL reported experimental values to new values based on use of modern calibration standards, and we also provide uncertainty assessments on the data, see Table I. This work is reported in more detail in a laboratory report by MacInnes *et al.* [104]. The measurements are reported in ratio to ^{235}U fission at the same location, a traditional Los Alamos approach that has the advantage of not requiring an absolute measurement of the neutron fluence to use the data. It does require that we also model fission in MCNP, but because ^{235}U(n,f) is a standard and we have much experience modeling it in our criticality calculations, the associated uncertainties in this part of the calculation are rather small, less than about 2%.

The procedure we have gone through to update the original reported measured values is as follows. One aspect is that the original radiochemical measurements determined count rates from the activation product decays following an irradition, and to convert these to an absolute physical scale the original scientists performed concurrent irradiations in a 14.1 MeV neutron beam, where the 14.1 MeV cross section was "known", measuring the induced count rates there as well. This calibration process, using the known 14.1 MeV cross sections, set the

TABLE XII. Reaction rate measurements of ^{203}Tl$(n,2n)$ in the HEU Flattop-25 critical assembly traverse, 3/13/1961 (distance measured from center in cm).

Distance	Reaction	Measurement
0.01	^{203}Tl$(n,2n)/^{235}$U(n,f)	1.495E-03
1.02	^{203}Tl$(n,2n)/^{235}$U(n,f)	1.465E-03
3.7	^{203}Tl$(n,2n)/^{235}$U(n,f)	1.401E-03
5.16	^{203}Tl$(n,2n)/^{235}$U(n,f)	1.403E-03
6.31	^{203}Tl$(n,2n)/^{235}$U(n,f)	1.011E-03
9.62	^{203}Tl$(n,2n)/^{235}$U(n,f)	4.432E-04
14.75	^{203}Tl$(n,2n)/^{235}$U(n,f)	2.119E-04

TABLE XIII. Reaction rate measurements of ^{90}Zr$(n,2n)$ in the HEU Flattop-25 critical assembly traverse, 2/20/1961 (distance measured from center in cm).

Distance	Reaction	Measurement
0.4	^{90}Zr$(n,2n)/^{235}$U(n,f)	4.778E-05
1.03	^{90}Zr$(n,2n)/^{235}$U(n,f)	5.153E-05
3.69	^{90}Zr$(n,2n)/^{235}$U(n,f)	4.678E-05
5.6	^{90}Zr$(n,2n)/^{235}$U(n,f)	4.004E-05
6.32	^{90}Zr$(n,2n)/^{235}$U(n,f)	3.432E-05
7.7	^{90}Zr$(n,2n)/^{235}$U(n,f)	2.277E-05
12.78	^{90}Zr$(n,2n)/^{235}$U(n,f)	1.017E-05

scale for the historical reported values. But since our knowledge of the 14.1 MeV cross sections has changed since the 1960s and 1970s, we update the original reported data to our new 14.1 MeV cross sections. Table IV shows the historical cross sections assumed as well as the modern ENDF/B-VII.1 values we have calibrated against. A second aspect is that we believe our historical radiochemical estimates of ^{235}U fission (in a fission spectrum) were too high by 2%, as discussed by Selby [86], and therefore our updated values account for this change.

Table V gives measured data in the center of the Jezebel assembly, a plutonium sphere. Table VI gives measured data in the center of the Flattop-Pu assembly, a plutonium core surrounded by depleted uranium. Table VII give measured data in the center of the Godiva assembly, a highly-enriched uranium sphere. Table VIII give measured data in the center of the Flattop-25 assembly, a highly-enriched uranium core surrounded by depleted uranium.

The subsequent tables provide data through a traverse

TABLE XIV. Reaction rate measurements of ^{90}Zr$(n,2n)$ in the HEU Flattop-25 critical assembly traverse, 3/13/1961 (distance measured from center in cm).

Distance	Reaction	Measurement
0.01	^{90}Zr$(n,2n)/^{235}$U(n,f)	4.765E-05
1.02	^{90}Zr$(n,2n)/^{235}$U(n,f)	4.705E-05
3.7	^{90}Zr$(n,2n)/^{235}$U(n,f)	4.400E-05
5.16	^{90}Zr$(n,2n)/^{235}$U(n,f)	5.081E-05
6.31	^{90}Zr$(n,2n)/^{235}$U(n,f)	3.480E-05
9.62	^{90}Zr$(n,2n)/^{235}$U(n,f)	1.414E-05
14.75	^{90}Zr$(n,2n)/^{235}$U(n,f)	1.862E-05

TABLE XV. Reaction rate measurements of ^{191}Ir$(n,2n)$ in the HEU Flattop-25 critical assembly traverse, 8/18/1970 (distance measured from center in cm for samples co-located with the spectral index data shown in the following table).

Distance	Reaction	Measurement
1.1	^{191}Ir$(n,2n)/^{235}$U(n,f)	1.904E-03
0.96	^{191}Ir$(n,2n)/^{235}$U(n,f)	1.936E-03
3.66	^{191}Ir$(n,2n)/^{235}$U(n,f)	1.799E-03
5.02	^{191}Ir$(n,2n)/^{235}$U(n,f)	1.715E-03
5.76	^{191}Ir$(n,2n)/^{235}$U(n,f)	1.515E-03
8.36	^{191}Ir$(n,2n)/^{235}$U(n,f)	9.289E-04
11.0	^{191}Ir$(n,2n)/^{235}$U(n,f)	5.544E-04
14.8	^{191}Ir$(n,2n)/^{235}$U(n,f)	3.766E-04

TABLE XVI. Reaction rate measurements of ^{238}U(n,f) in the HEU Flattop-25 critical assembly traverse, 8/18/1970 (distance measured from center in cm for samples co-located with the iridium data in the previous table).

Distance	Reaction	Measurement
1.1	^{238}U$(n,f)/^{235}$U(n,f)	0.1485
0.96	^{238}U$(n,f)/^{235}$U(n,f)	0.1495
3.66	^{238}U$(n,f)/^{235}$U(n,f)	0.1455
5.02	^{238}U$(n,f)/^{235}$U(n,f)	0.1315
5.76	^{238}U$(n,f)/^{235}$U(n,f)	0.1144
8.36	^{238}U$(n,f)/^{235}$U(n,f)	0.0583
11.0	^{238}U$(n,f)/^{235}$U(n,f)	0.0361
14.8	^{238}U$(n,f)/^{235}$U(n,f)	0.0223

of Flattop-25 from the central region out into the tamper. Tables IX and X give data for ^{238}U$(n,2n)$ and (n,f). Tables XI and XII give data for ^{203}Tl$(n,2n)$. Tables XIII and XIV give data for ^{90}Zr$(n,2n)$. Tables XV and XVI give data for ^{191}Ir$(n,2n)$ co-located with ^{238}U samples used to measure the spectral index.